THE ROLE OF ACTIN POLYMERIZATION IN MODEL HIRANO BODY FORMATION

by

YUN DONG

(Under the Direction of Marcus Fechheimer and Ruth Furukawa)

ABSTRACT

Hirano bodies are paracrystalline filamentous actin inclusions associated with multiple neurodegenerative diseases. The mechanism(s) of Hirano body formation remains largely unknown. Model Hirano bodies generated in *Dictyostelium* were utilized to identify their protein components and formation mechanism. From proteins identified in model Hirano bodies by mass spectrometry, mitochondrial proteins, profilin I and the Arp2/3 complex were further investigated. Mitochondria were not present in model Hirano bodies. Knockdown of profilin I reduces the size of model Hirano bodies. Inhibition of the Arp2/3 complex activity by CK666 reduced model Hirano body formation. When HSPC300, a subunit of an Arp2/3 complex activator, was knocked out, cells could not form model Hirano bodies. In contrast, when WASH, another Arp2/3 complex activator was knocked out, cells formed model Hirano bodies. These findings reveal that de novo actin polymerization is a key aspect of model Hirano body formation.

INDEX WORDS: Hirano bodies, Arp2/3 complex, HSPC300, WASH, Profilin, CK666, *Dictyostelium*.

THE ROLE OF ACTIN POLYMERIZATION IN MODEL HIRANO BODY FORMATION

by

YUN DONG

B.S., Peking University, China, 2011

A Thesis Submitted to the Graduate Faculty of The University of Georgia in Partial Fulfillment of the Requirements for the Degree

MASTER OF SCIENCE

ATHENS, GEORGIA

2015

THE ROLE OF ACTIN POLYMERIZATION IN MODEL HIRANO BODY FORMATION

by

YUN DONG

Major Professor: Marcus Fechheimer
Ruth Furukawa

Committee: Claiborne Glover
James Lauderdale
Walter Schmidt

Electronic Version Approved:

Julie Coffield
Interim Dean of the Graduate School
The University of Georgia
May 2015

ACKNOWLEGEMENTS

I would like to first thank my husband, Fan Yang, for being gentle, considerate, supportive and comforting. Without him or his tens of times of flying between Los Angeles and Athens, GA in these four years, I might not have been able to survive this whole process. I would like to also thank my parents for their support.

I would especially thank Dr. Ruth Furukawa and Dr. Marcus Fechheimer for their support, guidance, inspiration and all the suggestions on my life decisions. I could not have achieved all these without them. Particularly, I would like to thank their emphasis on details and critical thinking, which will help me a lot no matter what career path I finally choose.

I would like to thank my committee, Dr. Claiborne Glover, Dr. James Lauderdale and Dr. Walter Schmidt, for the suggestions on my project and the training on my scientific thinking. I would also like to thank Dr. Jacek Gaertig for his help during the early phase of my project, Dr. Scott Dougan for all kinds of help, and also all the other professors in CBIO that have questioned me to help me think deeper about the project.

I would like to thank Dr. Robert Insall and Dr. Angelika Noegel, for kindly sending some of the strains, plasmids and antibodies that are critical to this project. I would not be able to obtain my results without all these.

I would also thank my lab mate and friend Dr. Matt Furgerson, for all the help, support and encouragement. Also thanks to my lab mates Will Spears, Connor Sweetnam, Parker Evans, Sandip Manhans, Allison Wood, Ali Bobo and Nelson May, my time in the lab has been fun and

satisfying. I feel so lucky to have met and worked with you guys, and have learned so much from all of you.

I would also thank my fellow students, especially my friends Zhibo Ma, Anthony Gresko, Dr. Yue Qian, and Alicia Hudson, for your help and the time we spent together. Also thank you to the staff of CBIO, especially Carrie Harden and Angie Holiday, for taking care of all kinds of issues and making my life so much easier.

TABLE OF CONTENTS

Pages

LIST OF TABLES

Pages

LIST OF FIGURES

Pages

CHAPTER 1

INTRODUCTION AND LITERATURE REVIEW

Hirano bodies

Neurodegenerative diseases are a range of incurable conditions which are characterized by loss of structure or function of neurons. Some of these diseases have specific insoluble protein aggregations which are associated with loss of function, such as Alzheimer's disease (AD) with β-amyloid plaques [1] and neurofibrillary tau tangles [2], Parkinson's disease with Lewy bodies containing α-synuclein [3], and Amyotrophic Lateral Sclerosis (ALS) with the aggregation of TDP43 [4]. Most of the neurodegenerative disease specific protein aggregations share the characteristic of the enriched beta-pleated sheet structure, 'amyloid,' resulting from protein misfolding [5]. Research on these aggregations reveals crucial facts of the causes and propagation of the diseases [5], such as the cell-to-cell transmission of protein aggregation of tau [6], β-amyloid fibrils [7], or α-synuclein [8].

In addition to these protein aggregations, Hirano bodies (HBs) are also associated with neurodegenerative diseases. HBs were first discovered in the hippocampus in patients in Guam with amyotrophic lateral sclerosis – Parkinson dementia complex [9]. HBs have been observed in the hippocampus of autopsied brains from patients with diverse conditions including AD [10, 11] and Pick's disease [12], as well as in normal brains of elderly individuals [11]. HBs are predominantly found in the hippocampus, and also in other nerve cells, including cortical and anterior horn cells, and glial cells [13]. HBs are not specific to neurons, as they are also found in skeletal muscle [14].

HBs are ovoid or spindle-like eosinophilic inclusions, mainly composed of filamentous actin that can be stained with fluorescent phalloidin [15]. Ultrastructurally, HBs contain electron-dense lattice-like arrays of actin filaments measuring approximately 10 nm in diameter, which form the hallmark paracrystalline pattern [16]. However, HBs are different from the other protein aggregations associated with neurodegenerative diseases in some aspects. Compared to the other protein aggregations, actin, as the primary component of HBs, is not a β-pleated sheet enriched protein. Moreover, there is no evidence that the actin filaments in HBs are misfolded or that HBs can propagate between cells or different regions of the brain. In addition, the paracrystalline ultrastructure of HBs is unique among the protein aggregations. This evidence indicates that HBs are naturally different from the other disease specific protein aggregations.

There are also actin-cofilin rods that are associated with neurodegeneration and are more comparable to HBs in that they are composed primarily of F-actin [17, 18]. Cofilin is an actin regulator that severs F-actin at a low or medium cofilin/actin ratio due to a twist it induces on the filament [19]. Cofilin nucleates actin and even stabilizes actin filaments at a high cofilin/actin ratio [18, 20-22]. Thus, the actin-cofilin rods formed are saturated with cofilin and are not stained by fluorescent phalloidin [23-25]. In comparison to HBs, actin-cofilin rods lack the paracrystalline F-actin ultrastructure, and often form in neuronal processes instead of the cell body, blocking the trafficking along the neurites [26]. Moreover, it is known that actin-cofilin rods can be induced by physiological stress factors such as microischaemia, glutamate excitotoxicity, ATP depletion or oxidative stress [24]. It is undecided if the rods are intermediates in the formation of other aggregations [18]. Comparatively, the mechanisms of induction and formation of HBs are poorly understood.

Our understanding of the physiological function of HBs also continues to evolve. Initially, it was thought that HBs may not have cytopathological significance [27], since HBs are not specific to a certain cell type, and that HBs occur throughout life in subjects not diagnosed with neurodegenerative diseases [28]. However, other evidence suggests the opposite. The number of HBs significantly increases in stratum pyramidale of the hippocampi of patients with AD, compared to the normal individuals at a similar age [10, 11]. In normal individuals, HBs accumulate in stratum lacunosum up to the third decade of their life and then decrease, while in stratum pyramidale they build up more gradually and peak in the 8^{th} and 9^{th} decade, with a substantial increase for AD patients [11]. HBs were also found to colocalize with other proteins associated with neurodegenerative diseases, such as AICD and tau for AD (see Table 1.1). Moreover, HBs are also associated with proteins with diverse functions in the cytoskeleton, cell signaling, or transcription regulators, which could have some implications in the mechanisms of formation and effects of HBs (see Table 1.1). Taken together, HBs could be significant for cell physiology and associated with neurodegenerative diseases. Therefore, a thorough investigation of the cause(s) and effect(s) of HBs is necessary. However, initial investigations on HBs had been limited to autopsy specimens. Thus, a cellular model for HBs is essential for further research of HBs.

Formation of model Hirano bodies by introducing an altered form of a *Dictyostelium* actin binding protein

Cell models of HBs were created by introducing a carboxyl-terminal fragment (CT), the residues 124-295 of an actin binding protein, ABPB (ABP34), from the cellular slime mold *Dictyostelium*. These model HBs had paracrystalline F-actin ultrastructure and were formed in *Dictyostelium* and other mammalian cell lines [29, 30]. Model HBs were shown to colocalize

with the proteins found in HBs in autopsy specimens (see Table 1.2) [29-32]. These models provided methods to study the physiological roles of HBs in cells and animals, and substantially facilitated research on the possible role of HBs in neurodegenerative diseases.

Actin binding protein B (ABPB), a 34 kDa monomeric actin cross-linking protein, was first purified from *Dictyostelium discoideum* [33]. Three actin binding sites were identified by molecular dissection of recombinant forms of ABPB, as well as two calcium binding EF hands by cDNA sequence [34-36]. Based on the results of truncation studies, it was proposed that an N-terminal inhibitory domain of residues 1-76 inhibits the strong actin binding site, while the EF1 domain and the strong actin binding site form the intramolecular interaction zone that brings the inhibitory region into juxtaposition with the strong actin binding site [33, 35, 36]. With these regulation mechanisms, ABPB plays a significant role in the distribution and dynamic behavior of the actin cytoskeleton important for cell growth and locomotion in *Dictyostelium* [37].

It has been proposed that the gain-of-function of F-actin binding and loss of calcium regulation of CT induced the formation of model HBs [29]. Another mutant of ABPB, ΔEF1, which has a mutation in the first putative EF hand, activated F-actin binding and induced model HBs, supported this hypothesis [38]. However, E60K, in which the 60^{th} amino acid in the N-terminal inhibitory domain is mutated from a glutamate to a lysine, induces model HBs while retaining calcium sensitivity comparable to wild type ABPB [17]. Therefore, the activated F-actin binding of mutant ABPB is essential for model HB formation, while the calcium insensitivity is not. Expression of these mutant forms has been used to generate model HBs in order to investigate the mechanism(s) of formation and physiological function(s) of HBs.

The physiological functions investigated using model HBs include protection against cell death and influence on synaptic function and long-term potentiation. Model HBs were found

colocalized with Amyloid precursor protein Intracellular C-terminal Domain (AICD) as well as the nuclear adaptor protein Fe65 in H4 cells [39]. AICD forms a multimeric complex with the scaffold protein Fe65 and transcription factor Tip60 which translocates into the nucleus and thus stimulates gene expression and apoptosis [40, 41]. Exogenous expression of amyloid precursor protein (APP) with either AICD or the C-terminal fragment of APP, c31, enhances cell death [42, 43]. Model HBs protect cells from AICD-induced cell death, possibly through down-regulation of Fe65-dependent transcription [39, 43]. Several wild type and mutant forms of tau induce synergistic cell death with AICD [44]. Model HBs decrease this synergistic cell death, except for the tau mutants that induce cell death independent of AICD [44]. This effect is associated with the function of the kinase GSK3β, whose constitutively active form reverses the reduction of cell death by model HBs with some of the variants of tau [44]. The presence of model HBs was both protective and induced synergistic cell death, indicating a complex physiological role for model HBs. For mice with CT expressed in the CA1 subregion of hippocampus, spatial working memory impairment developed with age [32]. Model HBs also affected synaptic function and long-term potentiation differently depending on the specific location in the hippocampus that they form [31, 32]. Model HBs induced in the CA3 subregion of the hippocampus in mouse affected presynaptic vesicle trafficking [31], while those induced in the CA1 subregion did not [32]. To summarize, HBs can promote or impede disease progression depending on context. The physiological effects of HBs are complicated and need further study.

In addition, the degradation and formation of model HBs were also investigated. Larger model HBs formed in autophagy mutants as well as colocalization of model HBs with an autophagosome marker protein in wild type cells but not in autophagy mutants indicates a role for autophagy in the degradation of model HBs [45]. Furthermore, chemical inhibition of the

proteasome pathway largely slowed down the turnover of model HBs, suggesting that the degradation of model HBs is a process involving multiple pathways including autophagy and the proteasome [45].

The pathways that are involved in HB formation are still mostly unknown. The actin associated motor protein myosin II and tubulin were found to be relevant to model HB formation in *Dictyostelium* [17]. Using nocodazole and blebbistatin to inhibit microtubules and myosin II, respectively, model HBs were still able to form, but the size distribution of model HBs was different, suggesting the contribution of microtubules and myosin II to model HB formation [17].

The composition of model HBs was also examined to gain insight into the possible mechanism(s) of model HB formation and function. Model HBs were purified by iodixanol density gradients to investigate the components of model HBs. The fraction containing model HBs was determined by comparison to samples similarly processed from wild type cells [Shahid-Salles, Furukawa, Wells and Fechheimer, unpublished]. Mass spectrometry was performed to characterize the proteins associated with the density gradient fraction that model HBs were in [Shahid-Salles, Furukawa, Wells and Fechheimer, unpublished]. A list of the identities of the proteins was generated by analysis of the data using the genome of *Dictyostelium* (Table 1.3). In this list, there are proteins from cell membrane, cytosol, ribosome and mitochondria, as well as those from cytoskeleton [Shahid-Salles, Furukawa, Wells and Fechheimer, unpublished]. Nevertheless, some of the proteins might be contaminants of the same density as the model HBs. However, considering that actin is the primary component of HBs, the proteins in the list that are associated with the actin cytoskeleton are more likely to be authentic components of HBs rather than contaminants.

In summary, actin inclusions induced by altered forms of *Dictyostelium* actin binding protein ABPB make good models to study the physiological function, degradation and formation of HBs. However, the proteins involved in HB formation are still yet to be definitely determined. We hypothesize that actin related proteins found from mass spectrometry in model HBs play roles in HB formation. To further narrow down our scope, the proteins that are associated with actin polymerization are placed as our priority for further investigation.

Actin Polymerization

As one of the most plentiful and the most highly conserved proteins, actin plays key roles in cell physiology. It is one of the primary constituents of the actin based cytoskeleton, which participates in a variety of important processes such as cell migration, vesicular trafficking, and cell division. For example, actin dynamics play a key part in the navigation of the growth cone that leads growing axons to synaptic targets [46]. In this process, the assembly, turnover, and interaction with other actin filaments drive the protrusion and withdrawal of filopodia and lamellipodia [47]. Therefore, regulation of actin polymerization and depolymerization is the key to understand such processes [47].

The actin filaments are polarized with a pointed end and a barbed end which can be shown when the filament is decorated with the globular heads of myosin [48]. At the same actin monomer concentration, actin filaments grow faster at the barbed end (plus end) than the pointed end (minus end) [49]. Hydrolysis of ATP that binds to each actin monomer promotes release of the monomer from the filament. In addition, there are actin associated proteins that regulate the assembly or disassembly of actin filaments. To initiate a new filament, actin monomers have to first nucleate to form a stable trimer because of the instability of actin dimers [50]. The strong kinetic barrier to nucleation is overcome with the assistance of a variety of actin-nucleating

proteins, including formins, tandem-monomer-binding nucleators, and Arp (Actin related protein) 2/3 complex [50]. These proteins have some similarities, but more importantly have different effects on nucleation mechanisms and functions.

The Arp2/3 complex is the primary powerhouse of actin filament polymerization [47]. It is composed of seven evolutionarily conserved subunits, with Arp2 and Arp3 being similar to actin in sequence and structure, while the other five are unique [51]. It has been well established that the Arp2/3 complex is critical for the formation of branching actin filaments, in which it binds to the side of an existing filament and initiates the daughter filaments at a 70 ° angle [52, 53]. Structural information has revealed that Arp2 and Arp3 form an active dimer that serves as the base of polymerizing daughter filament branching from the mother filament, thus generating a network of actin filaments [52, 54]. As a result, the Arp2/3 complex has been well accepted to play a role in membrane trafficking and cell division, and most importantly, as the primary driver of formation of lamellipodia, which are sheet-like cell protrusions supported by the actin filament network [55, 56]. Altogether, the Arp2/3 complex is a vital factor in actin dynamics, but its role in different cell physiological processes remains to be clarified.

Regulation of the Arp2/3 complex is also at the forefront of current research, which at times is controversial, though some consensus has been established [47, 50]. The nucleation activity of Arp2/3 complex by itself is inefficient, requiring Nucleation Promoting Factors (NPFs) to be activated. NPFs are classes of proteins, of which the best known is the Wiskott-Aldrich Syndrome Protein (WASP), that contain WCA domains which consist of G-actin binding WASP homology 2 (WH2) peptides and Arp2/3-binding central/acidic (CA) sequences [50]. Binding of proteins containing WCA domains with the Arp2/3 complex along with actin monomers promote a conformational reorganization of the Arp2/3 complex, resulting in a dramatic increase of its

nucleation activity [57]. NPFs share the WCA domains at the C-terminus, with different lengths of CA sequence to induce differential activation of the Arp2/3 complex activity, while having unique N-termini that can be regulated by different proteins [58]. In this way, the Arp2/3 complex can play its role in different cell processes, and is fine tuned to meet different functional requirements instead of being regulated by simple on-off switches.

Many NPFs are also WASP family proteins, including Wiskott–Aldrich-syndrome proteins (WASPs), SCAR/WAVEs (Suppressor of cAMP Receptor, obtained through *Dictyostelium* genetics, or WASP and Verprolin homologous protein, since it is homologous with WASP), and WASH (WASP and SCAR homologue) [47]. They regulate different processes, and have their own mechanisms of activation. For example, WASPs regulate cell migration and endocytic processes at the plasma membrane [47]. They are activated by Cdc42 to remove the autoinhibition on WCA domains [59]. SCAR/WAVEs, however, are regulated by the other members of the five-membered Wave Regulation Complex (WRC), including Abi, HSPC300, Nap1 and PIR121 [47]. Within the WRC, the WCA domains of WAVE are sequestered. WRCs are recruited to the membrane by upstream signals, and triggered to release WAVE in order to activate Arp2/3 complex [60]. WRCs are able to interact with a variety of ligands, including small GTPases, kinases, acidic phospholipids, and scaffolding proteins [61]. Recruiting of proteins such as profilin stimulates activity of Scar1, and thus affects activation of WRC [62]. Altogether, these findings suggest that the diverse mechanisms of regulation of NPFs enable the many roles of the Arp2/3 complex in cellular processes.

In addition to actin-nucleating proteins, actin dynamics is also regulated by actin monomer binding proteins. One of the universally found actin monomer binding proteins is profilin. Though profilin was named by keeping actin in “the form of pro-filamentous actin [63],”

profilin binding to actin monomer causes a stabilization of an enlarged nucleotide pocket on the surface of the latter. This enhances the exchange of bound ADP to ATP on actin monomers, leading to "a charging of G-actin with ATP [64-66]." Besides actin monomer, profilin also binds to the barbed end of F-actin, ARPs, phospholipids, and proteins containing poly-L-proline stretches, such as formins or WASP/WAVE family [66]. It was shown that by this binding, profilin regulates the distribution of G-actin between the nucleation systems of the Arp2/3 complex and the less abundant formins by inhibition of the Arp2/3 complex [67, 68]. Consequently, profilin is involved in the regulation of actin dynamics during cell locomotion, cytokinesis, embryonic development and morphogenesis [69]. The knock-out of profilin is lethal in many organisms [69].

In conclusion, the regulation of actin cytoskeleton is a sophisticated multi-layer network that involves countless players and various pathways [47]. A disturbance in a single protein could result in complicated phenomena, and generation of an actin inclusion, such as the HBs, could involve numerous proteins and even signals from other systems. In this investigation, we looked at the roles of several proteins involved in actin dynamics to provide information on HB formation.

The scope of this project

In order to look into the protein components of model HBs, we particularly purified the model HBs and used mass spectrometry to investigate their components. We proposed to verify that at least some of the proteins that were identified by mass spectrometry are components of model HBs (Table 1.3), since some of the proteins that were discovered in model HBs by mass spectrometry are possibly contaminants from the rest of the cell, due to the limitation of the purification method. We focused on the actin binding proteins since HBs are composed primarily

of F-actin. The Arp2/3 complex was investigated because of its pivotal role in actin nucleation. Profilin was selected for investigation since it maintains the pool of G-actin available for polymerization and prevents the spontaneous and pointed end polymerization [65, 70]. We also investigated HSPC300 and WASH for a possible pathway through which the Arp2/3 complex is activated. Last but not least, colocalization of mitochondria as a whole was inspected to verify their presence in model HBs or whether they were contaminants in the purification. This study should shed some light on the composition and the mechanism of formation of Hirano bodies.

Table 1.1. Proteins associated with Hirano bodies

Protein	Function	References
Actin (F-actin)	Cytoskeleton	[15, 71]
α-actinin	F-actin cross-linking protein	[71]
α-1-antichymotrypsin	Protease Inhibitor	[72]
C1q Complement Protein	Immune Response	[73]
C9orf72	Unknown Function	[74]
Caspase cleaved actin (Fractin)	Unknown function	[75]
Caspase cleaved Transactivation Response DNA-binding Protein 43 (TDP-43)	Unknown Function	[76]
c-Jun N-terminal Kinase/Stress Activated Protein Kinase (JNK/SAPKγ)	Cell Signaling	[77]
Coenzyme Q_{10} (Ubiquinine)	Electron transport chain	[78]
Cofilin	Actin binding protein	[79]
C-terminal fragment of β-APP (AICD)	Transcription regulator	[80, 81]
FAC1	Transcription repressor	[82]
Factor-Induced-Gene 4 (FIG4)	Vesicle trafficking phosphatase	[83]
Hippocampus acetylcholine neurostimulating peptide (HCNP)	Hormone	[75]
Importin α	Cytoplasmic-nuclear transport	[84]
Inducible nitric oxide synthase (iNOS)	Stress response	[85]
Leucine-rich Repeat Kinase 2 (LRRK2)	Cell Signaling	[86]
Lipoprotein Lipase (LPL)	Lipid Exchange	[87]
MAP1 and MAP2	Microtubule binding protein	[88]
Neurofilament subunits L and M	Cytoskeleton	[11]
P130 (retinoblastoma related protein)	Transcription regulator	[89]
Phosphorylated Tau (pTau-199/202)	Microtubule binding protein	[44]
PSD-95	Synaptic scaffold protein	[90]
Smad ubiquitination regulatory factor 1 (Smurf1)	E3 ubiquitin ligase	[91]
Small heat shock protein 27 (HSP 27)	Stress response	[92]
Serine-arginine protein kinase 2 (SRPK2)	Cell Signaling	[93]
Tau protein	Microtubule binding protein	[80, 94]
Transactivation Response DNA-binding Protein 43 (TDP-43)	Transcriptional repressor/Splicing	[95, 96]
Transforming growth factor β3	Hormone	[72]
Tropomyosin	Actin binding protein	[71]
Ubiquillin-1	Cytoskeleton scaffold	[74]
Vinculin	Actin binding protein	[71]

Table 1.2. Proteins colocalized with model Hirano bodies

Protein	**Function**	**References**
Actin	Cytoskeleton	[29, 30, 38]
COOH fragments of APP (AICD)	Transcription Regulator	[39, 43]
α-actinin	F-actin cross-linking protein	[30, 38]
Cofilin	Actin binding protein	[29, 30]
Elongation Factor 1α (eEF-1α)	Translation	[29]
Importin α	Cytoplasmic-nuclear transport	[30]
Myosin II	Motor protein	[29 , 30]
Talin	F-actin cross-linking protein	[30]
Tau	Microtubule binding protein	[30, 43]
Tropomyosin	Actin binding protein	[30]
Ubiquitin	Protein degradation	[30]
Vinculin	Actin binding protein	[30]
Zyxin	Focal adhesions	[30]

Adapted from [30]

Table 1.3. Protein components of model Hirano bodies identified by mass spectrometry

	Protein	Department
1.	α-actinin	Cytoskeleton
2.	Arp 3	Cytoskeleton
3.	Arp2/3 p21	Cytoskeleton/actin
4.	Hisactophilin I	Cytoskeleton
5.	Myosin II heavy chain	Cytoskeleton
6.	Profilin 1	Cytoskeleton
7.	RAS-related rac 1A	Cytoskeleton
8.	SgcA	Cytoskeleton/actin
9.	Coronin	Cytoskeleton
10.	6-phosphofrutokinase	Cytosol
11.	20S proteasome beta	Cytosol
12.	H5 hydrolase	Cytosol
13.	Homogentisate 1,2 dioxygenase	Cytosol
14.	PI3 kinase	Cytosol
15.	Polyketide synthase	Cytosol
16.	Glucose-regulated protein 94 (HSP90)	Golgi complex
17.	P-type ATPase, potential aminophospholipid	Golgi complex
18.	Annexin VII	Membrane
19.	ATPase subunit 1	Membrane/cytosol
20.	Copine III	Membrane
21.	Crystal protein precursor	Membrane
22.	Gp130 glycoprotein130	Membrane
23.	guanine nucleotide-binding protein β	Membrane
24.	Protein Kinase C interacting protein	Membrane
25.	Rh-like glycoprotein	Membrane
26.	Vacuolar proton ATPase 100kDa subunit	Membrane/cytosol
27.	Vacuolar proton ATPase 41kDa subunit	Membrane
28.	Chaperonin 60	Mitochondria/cytosol
29.	Cysteine proteinase	Mitochondria
30.	Cytochrome c oxidase Polypeptide V	Mitochondria
31.	Dihydrolipoamide succinyltransferase	Mitochondria
32.	Glucose-6-1-dehydrogenase	Mitochondria
33.	Isocitrate dehydrogenase	Mitochondria/cytosol
34.	NADH-dehydrogenase subunit 7	Mitochondria
35.	NADH-ubiquinone oxidoreductase	Mitochondria
36.	Nucleoside-diphosphate kinase	Mitochondria
37.	porin	Mitochondria
38.	Succinate dehydrogenase flavoprotein subunit 1	Mitochondria
39.	Unknown proteasome subunit	Proteosome
40.	40S ribosomal protein S3	Ribosome
41.	40S ribosomal protein S4	Ribosome
42.	60S ribosomal L32	Ribosome
43.	60S ribosome	Ribosome
44.	EF1 alpha	Ribosome
45.	Major vault protein-alpha	Vault particle
46.	propinyl-CoA carboxylase β	Vesicle, phagocytic

CHAPTER 2

THE ARP2/3 COMPLEX AND PROFILIN I ARE CRUCIAL IN MODEL HIRANO BODY FORMATION[1]

[1] Dong, Y., S. Shahid-Salles, L. Wells, R. Furukawa and M. Fechheimer. To be submitted.

Abstract

Hirano bodies are paracrystalline filamentous actin inclusions associated with multiple neurodegenerative diseases and normal aging, but the mechanism(s) of Hirano body formation remains unknown. Model Hirano bodies generated in *Dictyostelium* by expressing altered forms of an actin binding protein were utilized to identify its protein components and formation mechanism. The model Hirano bodies were purified and examined by mass spectrometry. From the proteins identified, mitochondria proteins, profilin I, and the Arp2/3 complex were further investigated. Mitochondria were not present in model Hirano bodies. Knockdown of profilin I reduces the size of model Hirano bodies. Inhibition of the Arp2/3 complex activity by CK666 reduced model Hirano body formation. When HSPC300, a subunit of an Arp2/3 complex activator, was knocked out, cells could not form model Hirano bodies. In contrast, when WASH, another Arp2/3 complex activator was knocked out, cells formed model Hirano bodies. These findings reveal de novo actin polymerization as a key aspect of model Hirano body formation.

Introduction

Neurodegenerative diseases are a range of incurable conditions which are characterized by loss of structure or function of neurons. Some of these diseases have specific insoluble protein aggregations which are associated with loss of function, such as Alzheimer's disease (AD) with β-amyloid plaques [1] and neurofibrillary tau tangles [2], Parkinson's disease with Lewy bodies containing α-synuclein [3], and Amyotrophic Lateral Sclerosis (ALS) with the aggregation of TDP43 [4]. Actin inclusions are also found in neurodegenerative diseases, such as Amyotrophic Lateral Sclerosis, Parkinson's disease and Alzheimer's disease (AD), in the form of Hirano bodies and actin-cofilin rods [9, 15, 71, 97]. Hirano bodies are eosinophilic cytoplasmic inclusions that are primarily composed of F-actin, with an electron dense paracrystalline

ultrastructure [15, 16]. Hirano bodies colocalize with actin-binding proteins as well as proteins that are significant for neurodegenerative diseases, such as tau in AD. [71, 94]. However, since investigation of Hirano bodies is limited to postmortem tissues, the mechanism of Hirano body formation is largely unknown.

A model for Hirano bodies was developed by expressing altered forms of a 34 kDa *Dictyostelium* actin-binding protein, ABPB, in systems such as *Dictyostelium* cells and mammalian cell lines [17, 29, 30]. The C-terminal fragment (amino acids 124-295, CT), or the point mutation of E60 to lysine (E60K) of ABPB, show enhanced actin-binding affinity and induce inclusions with paracrystalline structures that resemble Hirano bodies [17, 29]. These inclusions also colocalize with proteins that were shown to colocalize with Hirano bodies in postmortem tissues [30]. Enhanced actin filament cross-linking and the inhibition of actin filament turnover were shown to be crucial to model Hirano body formation [17]. Thus, investigations of model Hirano bodies are useful for study of possible physiological effects and the mechanism of formation of Hirano bodies in neurodegenerative diseases [31, 32, 39, 43, 44]

In this study, we investigated the composition of model Hirano bodies and the roles of actin associated proteins in model Hirano body formation. Model Hirano bodies induced by myc-epitope tagged CT in *Dictyostelium* were partially purified by iodixanol density gradient centrifugation, and investigated by mass spectrometry to identify the proteins that are present in model Hirano bodies. Profilin I and Arp2 were identified by mass spectrometry and were chosen to be further investigated. Here we show that activity of the Arp2/3 complex or profilin I is critical to the size and/or numbers of model Hirano bodies. Our results suggest that actin polymerization, including actin nucleation, is crucial to the formation of model Hirano bodies.

Methods

Dictyostelium culture growth and transformation

All *Dictyostelium* strains were grown and maintained as axenic cultures in liquid media supplemented with appropriate antibiotics (see Table 2.1) at 20 ℃ and shaking at 150 rpm [98]. Cells were counted on a hemacytometer and passed every two days to a maximum density of $2X10^6$ cells/ml. For cells with the pVEII vectors [99], the media was supplemented with 1 mM folate and grown to a maximum density of $1X10^6$ cells/ml, in order to repress the expression of E60K-GFP driven by the discoidin promoter. No cells were maintained for more than 4 weeks.

To induce E60K-GFP expression by the discoidin promoter in pVEII, $5X10^6$ cells were plated in a 100 mm petri dish, washed two times with 17 mM phosphate buffer, and grown with 10 ml HL-5 media supplemented with appropriate antibiotics at 20 ℃ [100].

Dictyostelium cells were transformed with corresponding expression vectors (see Table 2.1) as previously described [101, 102]. Transformants were selected with appropriate antibiotics (see Table 2.1). The plasmids GFP-Arp2, HSPC300-GFP, and WASH-GFP were generous gifts from R. H. Insall. The strains [AS]proA, HSPC300$^-$, and WASH$^-$ were procured from the Dicty Stock Center [103]. G418 and blasticidin S were purchased from Life Technologies (Carlsbad, CA), and hygromycin B from EMD Millipore (Billerica, MA).

Drug Treatment

CK666 (Sigma-Aldrich, St. Louis, MO) was dissolved in DMSO to a stock concentration of 50 mM. Cells were incubated in HL-5 media for 6 hrs, 12 hrs and 18 hrs in the absence or presence of 100 μm CK666. For each sample with CK666, a solvent control incubated with equal concentration of DMSO for the same length of time was included.

Fluorescence Microscopy

Dictyostelium cells were prepared for immunofluorescence to visualize specific proteins and/or structures as previously described [104]. F-actin was labeled by TRITC-conjugated phalloidin. Mitochondria were labelled by MitoTracker® Red CMXRos (Invitrogen, Carlsbad, CA) with a working concentration of 200 nM for 30 min at 20 ℃ in live cells and followed by fixation. CT fragment of ABPB was labeled by primary antibody B2C generated in mouse and FITC-conjugated anti-mouse IgG [29]. Profilin I was labeled by primary antibody as a gift from A. A. Noegel, and FITC conjugated anti-mouse IgG [105]. Fluorescent-conjugated antibodies and phalloidin were obtained from Sigma-Aldrich, St. Louis, MO. Microscopy was performed using Applied Precision DeltaVision I microscope imaging system (GE Healthcare Bio-Sciences, Pittsburgh, PA). Images were assembled using Photoshop CS6 (Adobe Systems, San Jose, CA).

Determination of the size of model HBs and proportion of model HB forming cells

Microscopy images were taken in contiguous fields until a total of 200 model HBs were imaged. The total cell number in all the fields was also counted to calculate the proportion of cells that formed model HBs. The area of model HBs was measured using ImageJ [106]. Cells under each condition were repeated three times in independent experiments. The difference between the size distributions of model HBs in cells treated with CK666 and control cells was tested by exact test of goodness-of-fit. The difference between the proportion of cells that generated model HBs with or without the presence of CK666 was tested by Student's t-test. The difference between the size distribution of model HBs in [AS]proA and control cells was tested by Chi square test of goodness-of-fit.

Results

Mitochondria did not colocalize with model HBs

To verify whether mitochondria are in HBs or whether they were contaminants in the fraction containing model HBs, we induced the expression of E60K-GFP using the discoidin promoter for 24 hrs. The cells were stained with MitoTracker® Red CMXRos (Invitrogen, Carlsbad, CA), a live cell dye, and fixed. The mitochondria did not colocalize with model HBs in fixed cells (Figure 2.1). Thus, mitochondria and its associated proteins identified by mass spectrometry appear to be contaminants in the model HB purification. All mitochondrial proteins were eliminated from the list of possible proteins in model HBs identified by mass spectrometry.

Colocalization of the Arp2/3 complex with model HBs

Since the subunits of the Arp2/3 complex Arp3 and p21 (also named ARPC3) were identified by mass spectrometry, the presence of Arp2 and Arp3 in model HBs was tested. Cells with CT-myc constitutively expressed were transformed with GFP-Arp2 [107] and stained with TRITC-labeled phalloidin [29]. To also determine the localization of Arp3 compared to the model HBs, cells constitutively expressing GFP-Arp3 [107] were transformed with CT-myc and stained with TRITC-labelled phalloidin. GFP-Arp2 was enriched in model HBs (Figure 2.2). GFP-Arp3 localized at similar regions of cells as GFP-Arp2, and was enriched in model HBs (Figure 2.3). These results support that the Arp2/3 complex colocalizes with model HBs, consistent with the mass spectrometry data.

Inhibition of the Arp2/3 complex activity inhibits model HB formation

To determine the role of the Arp2/3 complex in model HB formation, we utilized an Arp2/3 complex inhibitor, CK666, since knockout of either Arp2 or Arp3 is lethal. It has been

shown that CK666 specifically inhibits the actin nucleation activity of the Arp2/3 complex [108]. A mechanism was proposed that CK666 inhibits Arp2/3 complex activity by preventing it from conformational reorganization crucial for activation [108]. However, it has never been used in *Dictyostelium*. Moreover, in most of the previous publications involving CK666, it was incubated with the cells for approximately 30 min [108, 109]. In contrast, it takes at least 3 hrs to see the small F-actin foci forming, and more than 6 hrs to see a significant number of model HBs with a considerable size [17, 110]. Therefore, it was necessary to test whether CK666 inhibits *Dictyostelium* Arp2/3 complex for a length of time comparable to model HB formation before utilizing it to investigate the role of Arp2/3 complex in model HB formation.

To determine if CK666 inhibits *Dictyostelium* Arp2/3 complex activity and the time span of efficacy, we incubated *Dictyostelium* cells constitutively expressing GFP-Arp3 with 100 μm CK666, with DMSO as the solvent control, or media, for different lengths of time, followed by fixation and staining with TRITC-labelled phalloidin to show the localization of F-actin. In agreement with published data, GFP-Arp3 colocalized with F-actin at the cortex and the lamellipodia in the controls (Figure 2.4) [107]. In contrast, in the cells incubated in the presence of CK666, the colocalization of F-actin and GFP-Arp3 was reduced, and GFP-Arp3 was not localized in the cortex or lamellipodia (Figure 2.4). This shows that CK666 inhibited the activity of the Arp2/3 complex in *Dictyostelium*, and this effect lasted for at least 18 hrs. Therefore, CK666 could be used as a tool to examine the role of the Arp2/3 complex in model HB formation.

Subsequently, E60K-GFP cells were induced in the presence or absence of 100 μm CK666. Cells were fixed and stained with TRITC-phalloidin to visualize the F-actin at 6 hrs, 12 hrs and 18 hrs after induction of model HBs as shown in Figure 2.5. The cells in the presence of

CK666 formed much fewer model HBs compared with the controls, consistent with the data that arp2/3 colocalized with the model HBs. Some of the model HBs that formed in the presence of CK666 showed abnormal morphology compared to those in the controls (Figure 2.5). To quantify this effect, we counted the proportion of cells with model HBs, and the size of model HBs in each of the samples. At each of the time points, compared with the controls, the proportion of cells that formed model HBs was dramatically lowered by 90% (Figure 2.6. $p < 1X10^{-7}$ for all three time points). Moreover, the distribution of area of model HBs was also changed significantly (compared to solvent control, $p < 0.01$ at 6 hr, $p < 0.001$ at 12 hr and at 18 hr. Figure 2.6). These trends were repeated in three independent experiments.

To rule out the possibility that the inhibition of model HB formation by CK666 was due to a non-specific inhibition, we washed out CK666 after 12 hrs of incubation and allowed the cells to recover for another 12 hrs with media under conditions for inducement of E60K-GFP. Following washout of CK666, model HBs formed in a significant proportion of cells (Figure 2.7). Thus CK666 did not destroy the pathway(s) of model HB formation, and the process of model HB formation can still be triggered. Therefore, CK666, which inhibits the Arp2/3 complex activity, also inhibits model HB formation and confirms that Arp2/3 is required for model HB formation in *Dictyostelium*.

Colocalization of the activators of the Arp2/3 complex, HSPC300 and WASH, with model HBs

Since the Arp2/3 complex is required for model HB formation, two of the Arp2/3 complex activators, HSPC300 and WASH, were examined to ascertain whether they also colocalized with model HBs. Cells constitutively expressing CT-myc were transformed separately with either HSPC300-GFP [111] or WASH-GFP [112] and followed by staining with TRITC-labelled phalloidin [29]. HSPC300-GFP and WASH-GFP showed localization analogous

to Arp2 or Arp3 (Figures 2.8 and 2.9). Moreover, both HSPC300-GFP and WASH-GFP were also enriched in model HBs (Figures 2.8 and 2.9). Together, these results suggest that model HB formation involves the activity of the Arp2/3 complex, and its activation by the NPFs including WASH and WRC, with HSPC300 as a subunit. Therefore, the roles of these proteins in model HB formation were investigated.

The role of HSPC300 and WASH in model Hirano body formation

Since HSPC300 and WASH colocalized with model HBs, studies of model HB formation in the knockout strains of HSPC300 and WASH were used to test the proposition that the Arp2/3 complex plays a part in model HB formation, and will indicate a possible pathway that the Arp2/3 complex is activated for the model HBs.

To determine if model HBs form in HSPC300 knockouts, we transiently transformed HSPC300$^-$ [111] with CT-myc under a constitutive actin promoter. We examined a large number of cells fixed different lengths of time after transformation, and didn't find any model HBs in cells that should have been expressing CT-myc (Figure 2.10). This indicates that HSPC300, and moreover the WRC, is critical for model HB formation through the regulation of the Arp2/3 complex.

However, when we transiently transformed WASH$^-$ [112] with CT-myc, actin inclusions formed in a substantial proportion of cells (Figure 2.11). These inclusions also colocalized with CT (Figure 2.11), which indicates that they are model HBs induced by expression of CT. Therefore, knockout of WASH does not have a significant influence on model HB formation.

The role of profilin I in model Hirano body formation

Since profilin I was also one of the actin cytoskeleton components of model HBs identified by mass spectrometry, we examined its colocalization with model HBs in CT-myc

expressing cells by immunofluorescence. Profilin I was enriched and colocalized well with the model HBs (Figure 2.12). This result verified the presence of profilin I in model HBs.

To determine if profilin I affects model HB formation, we transformed profilin I knockdown cells ([AS]proA) [105] with constitutively expressing CT-myc [29]. Transformed cells ([AS]proA-CT), [AS]proA and wild type cells with CT-myc expressed were immunoblotted to confirm that expression of profilin I was largely reduced (data not shown). Model HBs still formed in transformed cells (Figure 2.13). However, compared with wild type cells that expressed CT-myc (CT), model HBs that were formed when profilin I was knocked down were significantly smaller (Figure 2.14, $p < 0.001$). This result suggests that profilin I is involved in model HB formation.

Discussion

Hirano bodies are associated with aging and a variety of conditions, but the proteins that are necessary for HB formation are largely unknown. Model HBs were partially purified from *Dictyostelium* cells using iodixanol gradient centrifugation. Varying amounts of organelles including mitochondria and nuclei were also located in the same bands of density gradient with model HBs, and the samples were not further purified due to the instability of model HBs. The components of model HBs were identified by mass spectrometry and included proteins located in the cytoskeleton, cytosol, as well as in nuclei and mitochondria (Table 1.3). Thus, the presence of proteins from nuclei and mitochondria with model HBs in mass spectrometry might be impurities from those organelles in the density gradient bands and required verification. The result that mitochondria do not colocalize with model HBs (Figure 2.1) supports this possibility.

The major component of Hirano bodies is filamentous actin [15], which leads us to propose that actin regulating proteins included in the results of mass spectrometry, such as the

Arp2/3 complex and profilin, might indeed localize in HBs and play roles in model HB formation. However, some of actin associated proteins, such as ABP120, an actin cross-linking protein, showed little colocalization with model HBs [29]. Thus immunofluorescence is necessary to verify the colocalization between the proteins and model HBs.

The two subunits of the Arp2/3 complex, Arp2 and Arp3, showed colocalization with model HBs (Figures 2.2 and 2.3). This implied a role of the Arp2/3 complex in model HB formation. This result was reinforced by the significant reduction of model HB numbers, and the changes of model HB morphology when the cells were incubated with the small molecule CK666, a specific Arp2/3 complex inhibitor (Figures 2.5 and 2.6). These results show that the Arp2/3 complex plays a major role in model HB formation.

The Arp2/3 complex nucleates F-actin by binding at the sides of preexisting actin filaments, initiating actin filament branches at an angle of approximately 70 ° from the mother filament with Arp2 and Arp3 as the first two subunits of the daughter filament [52, 53]. With this in mind, our results suggest that in model HB formation, the Arp2/3 complex may be involved by initiating the F-actin polymerization. This indicates that the formation of model HBs involves not only the crosslinking of existing actin filaments [17], but also branching and de novo polymerization of filamentous actin. Considering the paracrystalline ultrastructure of HBs [16], it is possible that the Arp2/3 complex also plays a role in forming this pattern, as the actin inclusions formed when the Arp2/3 complex inhibited are much less dense than those in the control (Figure 2.5).

Since the activation of the Arp2/3 complex requires binding of the nucleation promoting factors (NPF), we investigated if model HBs form in HSPC300 or WASH knockout cells. No model HBs were found in transformed HSPC300 knockouts (Figure 2.10), but some were found

in transformed WASH knockouts (Figure 2.11). This suggests that the WAVE Regulation Complex (WRC), of which HSPC300 is a subunit [113], contributes to model HB formation. However, this does not exclude the possibility that WASH might play a comparatively minor role in model HB formation. WASH was shown to play an important role in exocytosis and vesicle trafficking [112], while WRC is involved in cell motility such as lamellipodia dynamics [60]. This indicates that WASH and WRC may mediate distinct aspects of Arp2/3 complex functions from each other. Thus, formation of Hirano bodies is more likely to be regulated through the pathway with activation of the Arp2/3 complex by WRC than through WASH.

Since the WRC also needs to be activated to function, its main activator and recruiter Rac1 [61, 114], is potentially also present in model HBs according to our mass spectrometry data (Table 1.3). Thus, the results suggest that Rac1 is also upstream to model HB formation. In addition, it was previously shown that increased Rac1 activity is associated with the enhancement of actin polymerization induced by fibrillary amyloid beta peptide [115]. Moreover, WAVE was shown surrounding senile plaque in postmortem tissue, upregulated in tissues from AD patients, and colocalizing with tau in AD mouse models [116, 117]. Taken together, this suggests that the formation of HBs could be promoted by the pathology of neurodegeneration; it is possible that the pathway involves Rac1, WRC and the Arp 2/3 complex may also be upregulated to facilitate it.

The actin monomer binding protein profilin has been shown to increase the assembly rate of actin filaments by increasing the rate of exchange of ATP for ADP binding to G-actin, thus maintaining an actin-ATP pool available for polymerization [118]. Therefore, the presence of profilin enhances the dynamics of actin. Our results show that model HBs are significantly smaller when profilin I is knocked down in *Dictyostelium* (Figure 2.14). This indicates that

profilin enhanced assembly of F-actin and is critical to the size of the model HBs, highlighting the role of de novo actin polymerization in model HB formation.

The effect of profilin on model Hirano body formation also hints at other players in this process. Recent studies suggest that by binding G-actin, profilin indirectly competes with WASP [67]. Consequently, since profilin also facilitates the function of formins [67, 119, 120] and Ena/VASP [68], which favor unbranched actin filaments over branched actin networks, profilin steers the utilization of G-actin from the Arp2/3 complex towards the system comprised by formins and Ena/VASP [67, 68]. Considering our results that depletion of either functional profilin or Arp2/3 complex both inhibit formation of model Hirano bodies possibly due to the requirement of de novo filament formation, the role of formins and Ena/VASP in assisting the formation of Hirano bodies should also be investigated.

It has been reported that the crosslinking of filamentous actin [17], the transportation and clustering of small actin aggregations [110], and the stabilization of filamentous actin [45, 121] are critical for model HB formation. Our results here suggest that actin polymerization which is regulated by the Arp 2/3 complex and profilin, is also crucial for allowing the model HBs to form, indicating that they are likely to play a role in Hirano body formation of human nervous system. However, since the actin cytoskeleton is a complex and multilayer regulated dynamic system [47], there are possibly many more factors associated with this system that affect Hirano body formation. Future investigation is needed on how these aspects coordinate, and which proteins generate the signal to initiate this polymerization and crosslinking.

Table 2.1. Strains and plasmids used for transformation

Strains	**antibiotic resistance**	**promotor**	**plasmid**	**selectable marker for plasmid**
CT-myc [29]	G418	constitutive	GFP-Arp2 [107]	Hygromycin
			HSPC300-GFP [111]	Hygromycin
			WASH-GFP [112]	Hygromycin
GFP-Arp3 [107]	G418	constitutive	pUCBsrDBam, CT-myc [29]	blasticidin S
E60K-GFP [17]	G418	induced by deprivation of folic acid	N/A	N/A
[AS]proA [105]	G418	constitutive	pUCBsrDBam, CT-myc [29]	blasticidin S
HSPC300- [111]	blasticidin S	constitutive	CT-myc [29]	G418
WshA- [112]	blasticidin S	constitutive	CT-myc [29]	G418

Figure 2.1. Localization of mitochondria and model HBs in *Dictyostelium.* Cells were observed by differential interference contrast (DIC) microscopy (A), and by fluorescence microscopy using either MitoTracker® (C) to visualize mitochondria, or E60K-GFP (D). Mitochondria do not colocalize with model HBs (B). Instead, the model HBs are devoid of mitochondria (B). Thus mitochondria do not colocalize with model HBs. Scale bar = 10 μm.

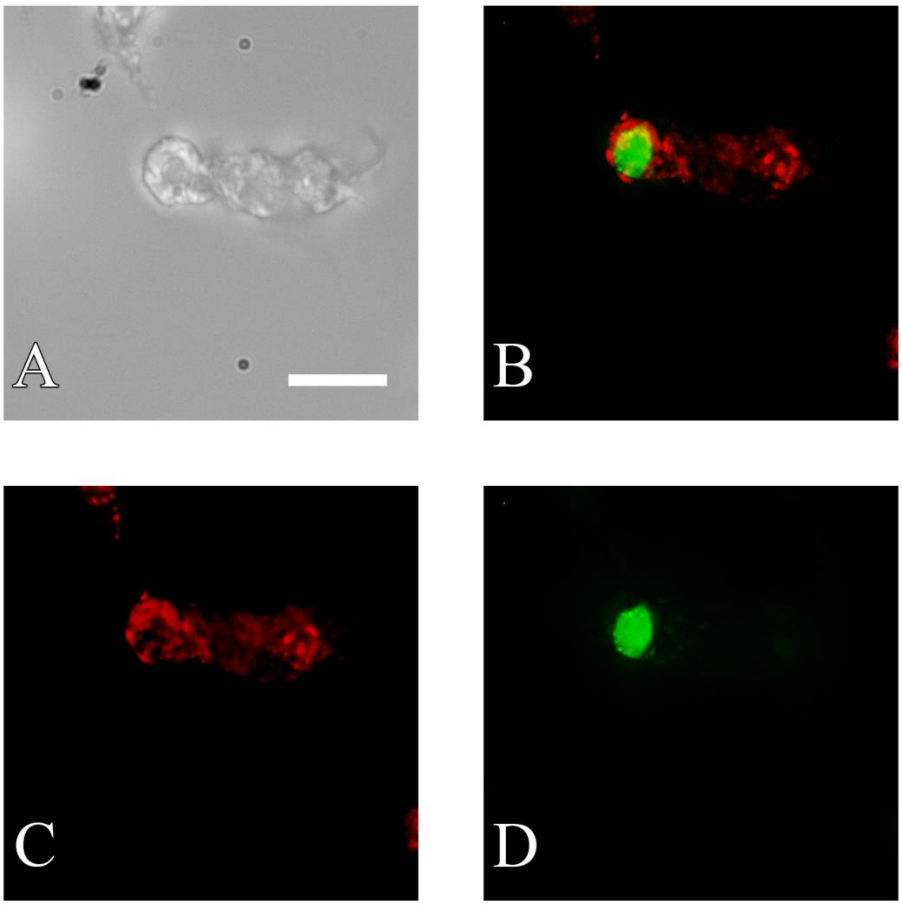
A
B
C
D

Figure 2.2. Localization of Arp2 and F-actin in *Dictyostelium* cells generating model HBs. Cells expressing CT-myc were transformed with plasmid to express GFP-Arp2, and were observed by DIC microscopy (A), and by fluorescence microscopy using either TRITC-phalloidin (C) to visualize F-actin, or GFP to visualize Arp2 (D). Arp2 is enriched in lamellipodia, and also model HBs generated by expressing CT-myc (B, D). Scale bar = 10 μm.

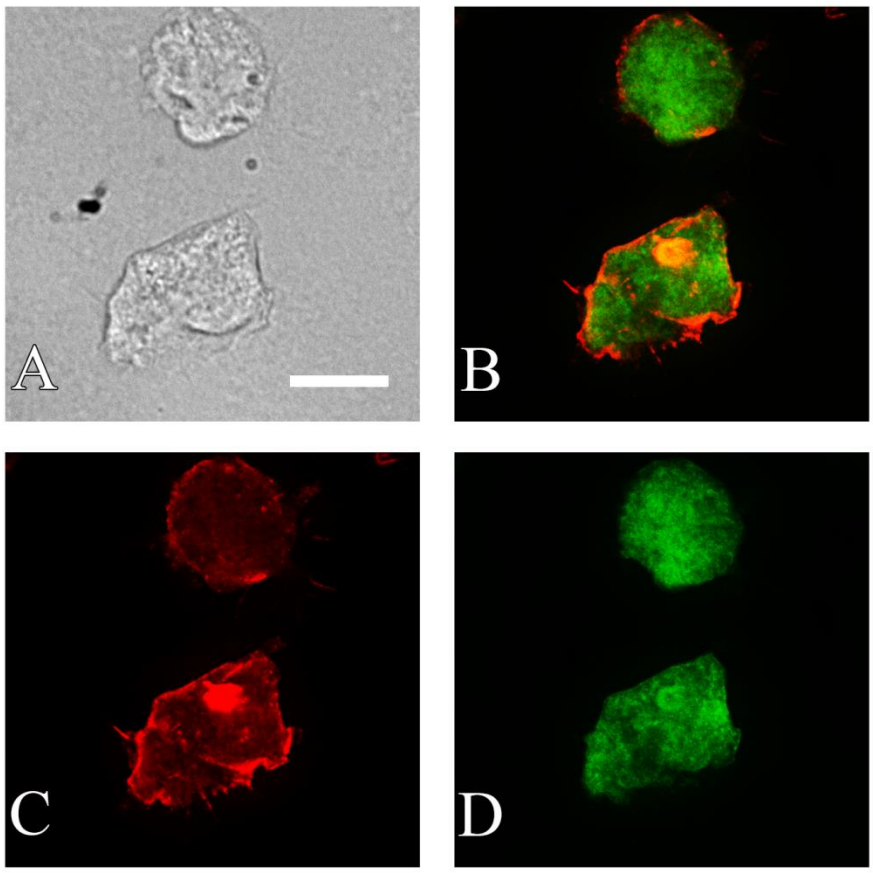
A
B
C
D

Figure 2.3. Localization of Arp3 and F-actin in *Dictyostelium* cells generating model HBs. Cells expressing GFP-Arp3 were transformed with plasmid to express CT-myc to generate model HBs. Cells were observed by DIC microscopy (A), and by fluorescence microscopy using either TRITC-phalloidin (C) or GFP to visualize Arp3 (D). Arp3 is enriched in model HBs generated by expressing CT-myc (B, D). Scale bar = 10 μm.

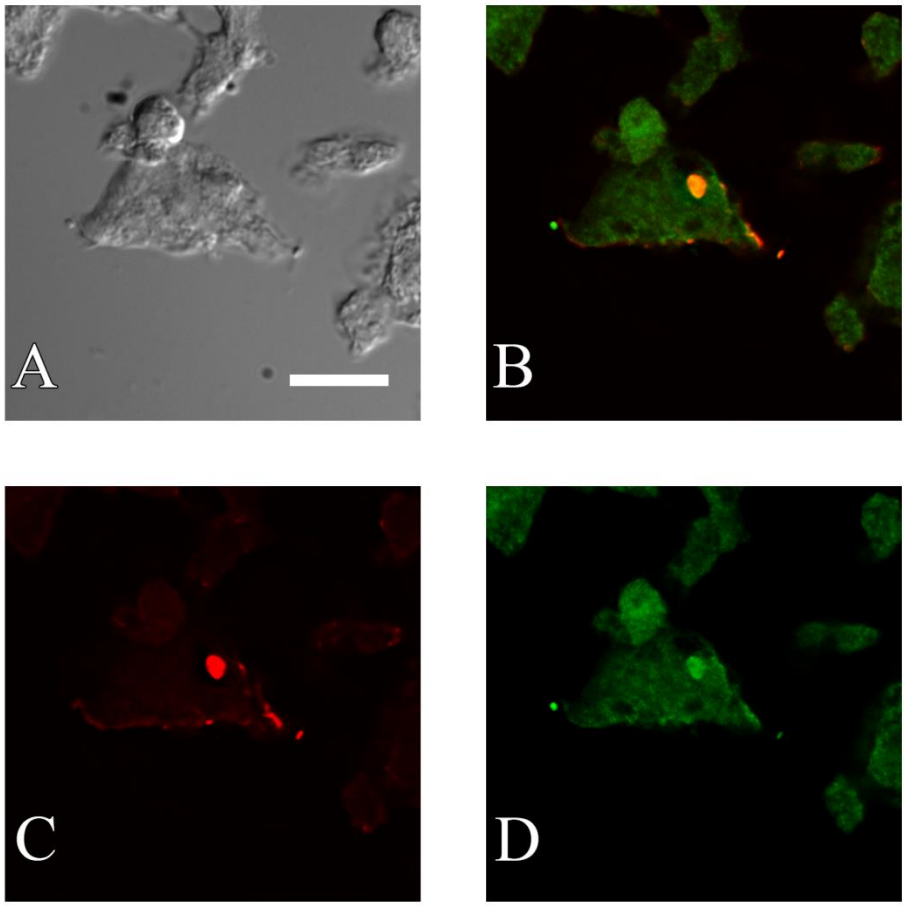
A
B
C
D

Figure 2.4. CK666 disrupts the localization of Arp3 and F-actin. GFP-Arp3 expressing cells were incubated and starved in the presence of either CK666 (left panel), or DMSO (middle), or plain media (right) for 18 hrs and examined by DIC microscopy (first row from the top), and by fluorescence microscopy using TRITC-phalloidin (second row) or GFP (third row). GFP-Arp3 is enriched at the cortex and especially lamellipodia, colocalizing with F-actin, in the cells with DMSO or plain media (middle and right). In contrast, this colocalization largely disappears in cells with CK666 (left). Arrows indicate the enrichments of GFP-Arp3 and F-actin. Scale bar =10 μm.

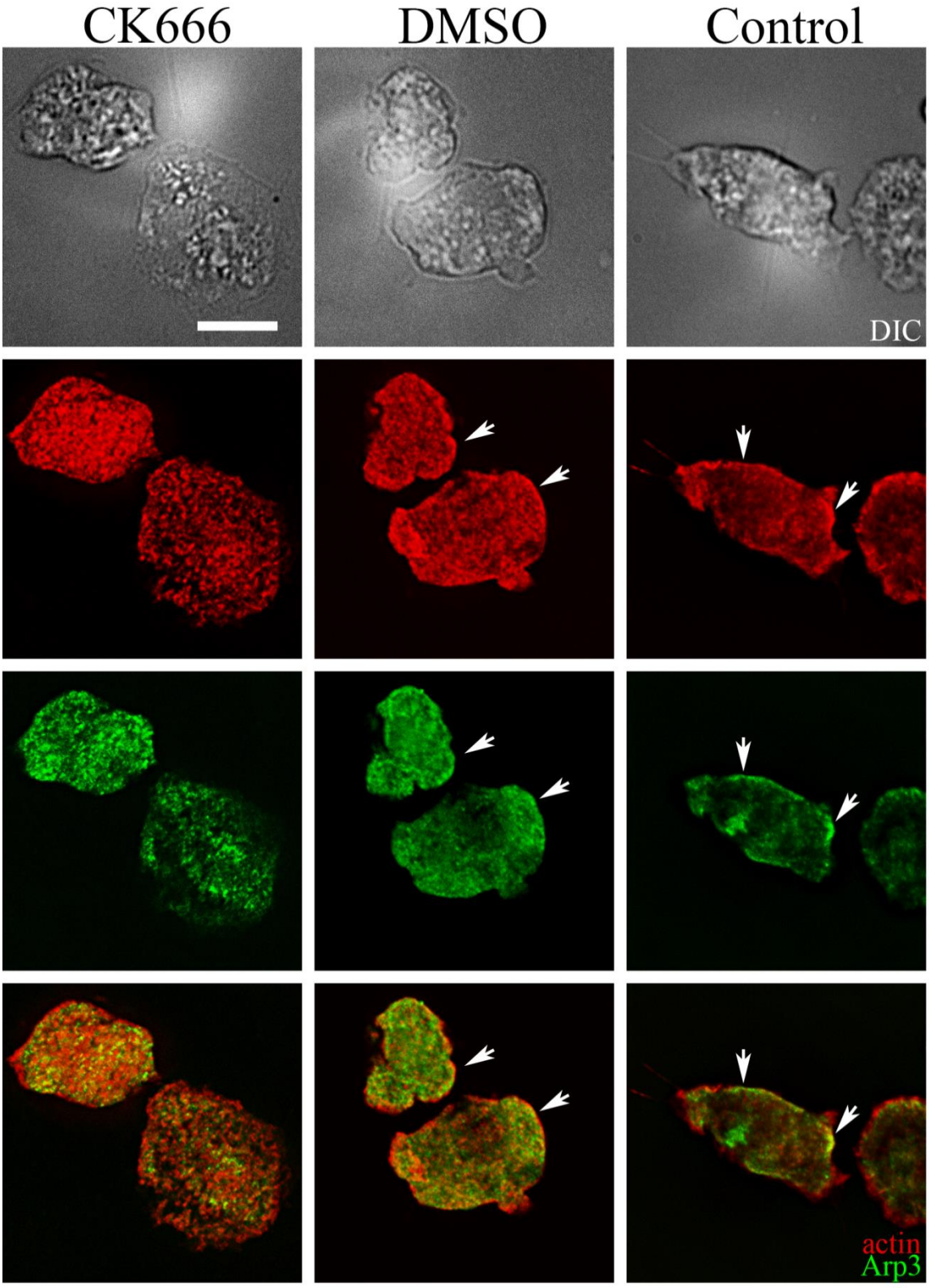
CK666
DMSO
Control
DIC
actin
Arp3

Figure 2.5. Model HB formation is inhibited by CK666. Cells were induced to express E60K-GFP, and were immediately incubated for 12 hrs with CK666 (left column), DMSO (middle column), or plain media (right column) and examined by fluorescence microscopy using TRITC-phalloidin (top row) or GFP (middle row). Compared with the controls, E60K-GFP aggregated when incubated with CK666 (middle left), but F-actin aggregations were less focused (top left). Scale bar = 10 μm.

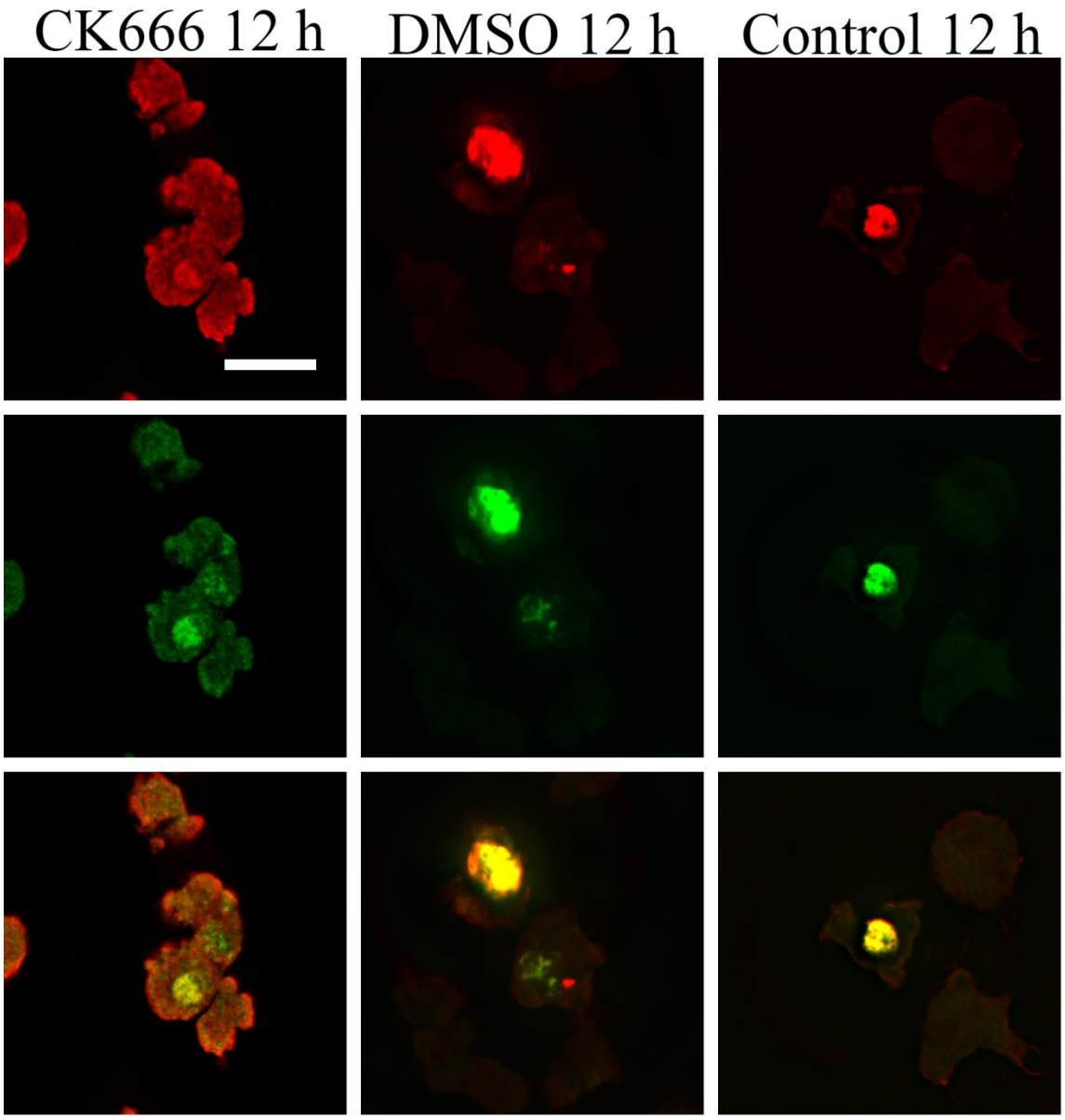
CK666 12 h
DMSO 12 h
Control 12 h

Figure 2.6. CK666 affects the distribution of model HB size and the number of cells that generate model HBs. The size distribution of model HBs was measured at 6 hrs (A), 12 hrs (B) or 18 hrs (C) of incubation with CK666 (green) after depletion of folic acid to induce expression of E60K, compared with cells incubated with DMSO (red) or plain media (blue) under the same condition to induce model HBs. The distributions of the model HB size were significantly changed ($p < 0.01$ at 6 hrs, $p < 0.001$ at 12 hrs and at 18 hrs). The proportions of cells that generated model HBs with or without CK666 were also counted, and compared with the control (D). The cells that produced model HBs were significantly reduced when incubated with CK666 ($p < 1X10^{-7}$ for all three time points).

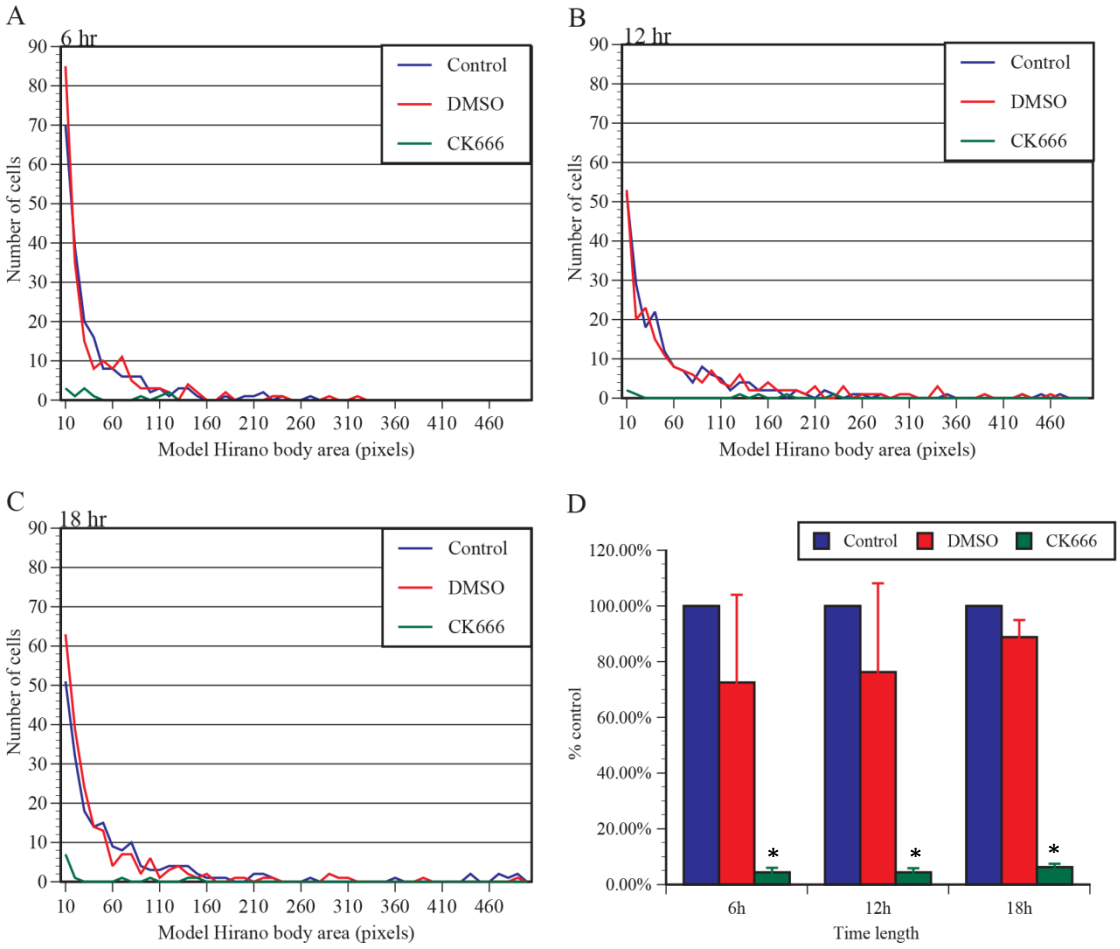
A
6 hr
Control
DMSO
CK666
Number of cells
Model Hirano body area (pixels)
B
12 hr
Control
DMSO
CK666
Number of cells
Model Hirano body area (pixels)
C
18 hr
Control
DMSO
CK666
Number of cells
Model Hirano body area (pixels)
D
Control
DMSO
CK666
% control
120.00%
100.00%
80.00%
60.00%
40.00%
20.00%
0.00%
6h
12h
18h
Time length

Figure 2.7. Model HBs form after CK666 was washed out. Cells were induced to express E60K-GFP and immediately incubated with CK666 for 12 hrs. They recovered in media after CK666 was removed for another 12 hrs (left panel). Cells that were induced to express E60K-GFP at the same time (middle panel) and at the time of wash out (right panel) were also observed as controls. All cells were examined by DIC (first row), and by fluorescence microscopy using TRITC-phalloidin (second row) or GFP (third row). Model HBs formed in a substantial amount of cells in all three samples. Scale bar = 15 μm.

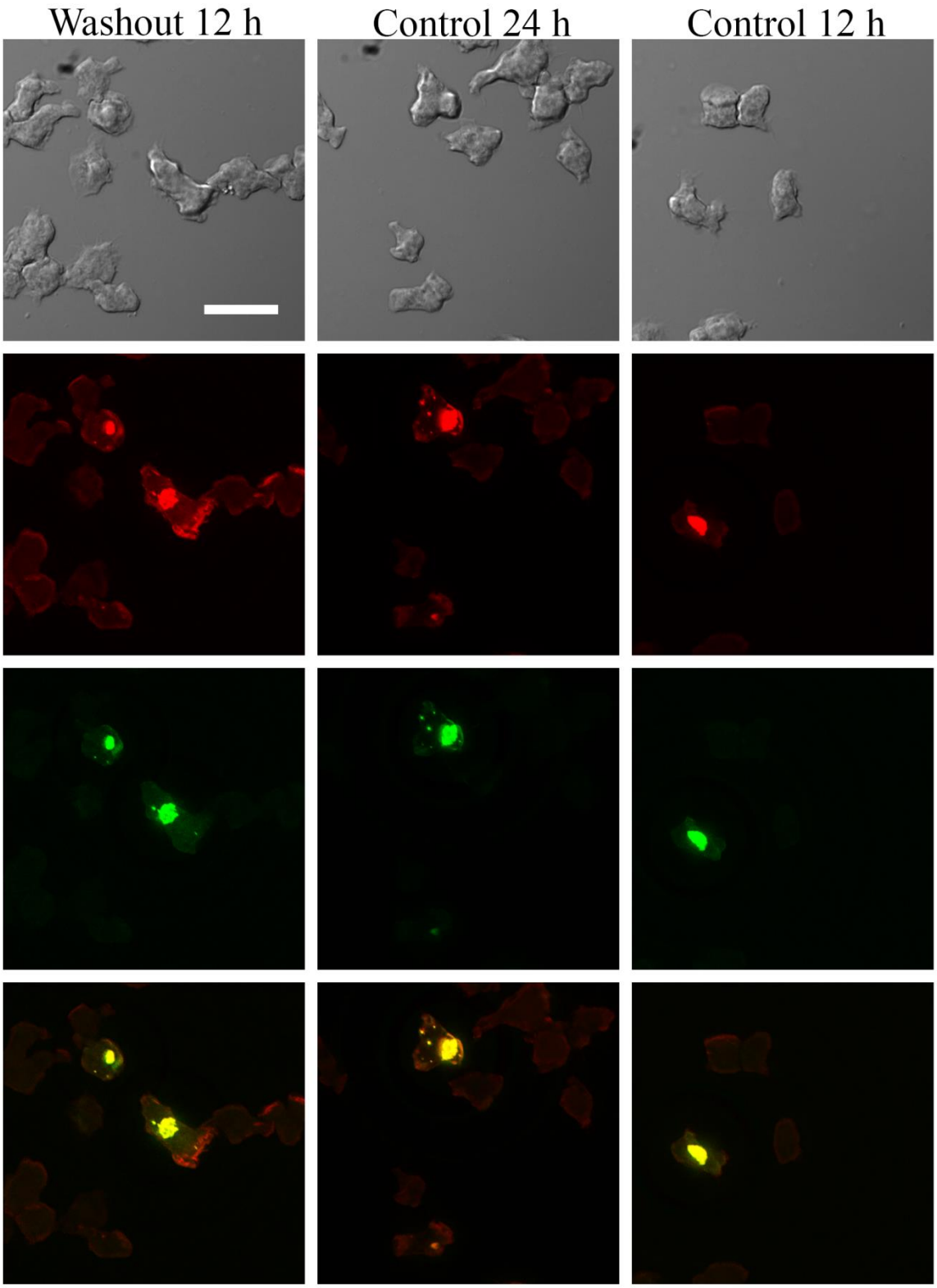
Washout 12 h
Control 24 h
Control 12 h

Figure 2.8. Localization of HSPC300 and F-actin in *Dictyostelium* cells generating model HBs. Cells expressing CT-myc were transformed with plasmid to express HSPC300-GFP, and were observed by DIC microscopy (A), and by fluorescence microscopy using either TRITC-phalloidin (C) or GFP (D). HSPC300 is enriched in model HBs (B, D). Scale bar = 10 μm.

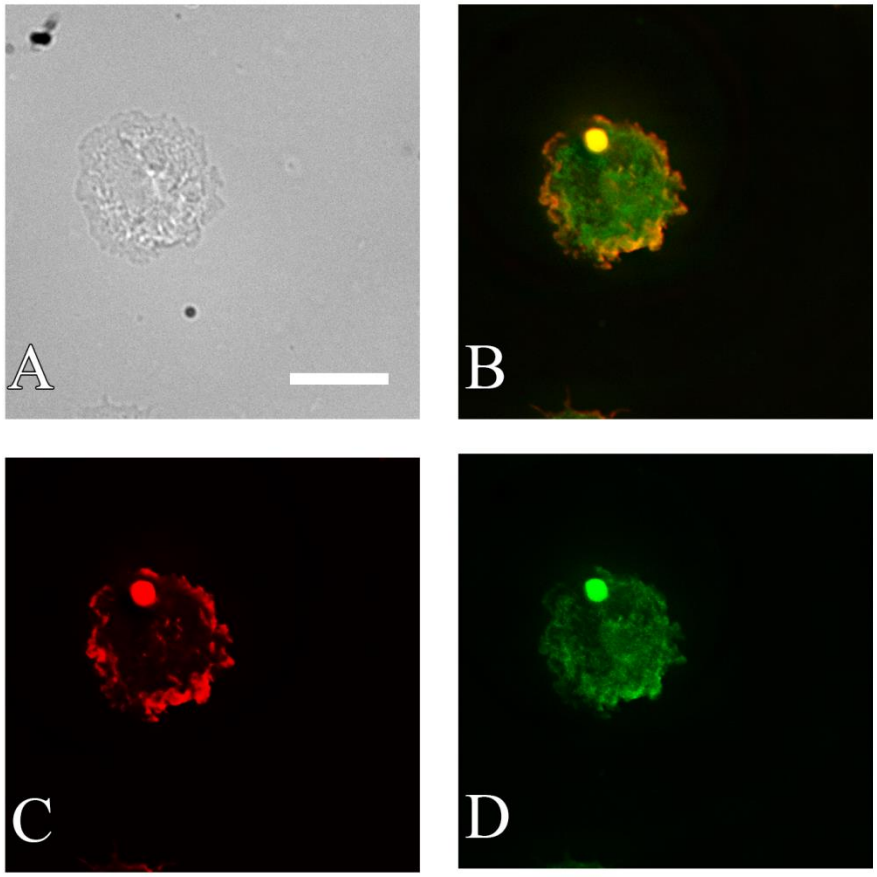
A
B
C
D

Figure 2.9. Localization of WASH and F-actin in *Dictyostelium* cells generating model HBs. Cells expressing CT-myc were transformed with plasmid to express WshA-GFP, and were observed by DIC microscopy (A), and by fluorescence microscopy using either TRITC-phalloidin (C) or GFP (D). WASH is enriched in model HBs (B, D). Scale bar = 10 μm.

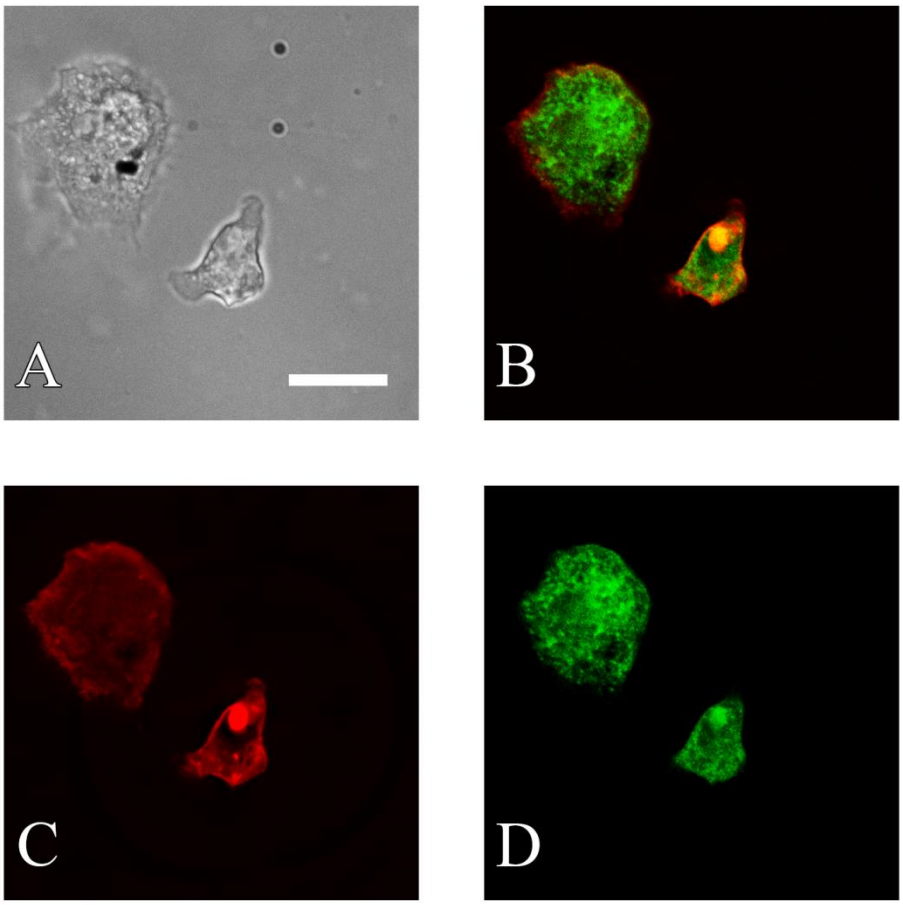
A
B
C
D

Figure 2.10. No model HBs form in HSPC300$^-$-CT-myc. HSPC300$^-$ transformed with CT-myc (left panel), and untransformed HSPC300$^-$ (right panel), were examined by DIC microscopy (first row from the top), and by fluorescence microscopy using TRITC-phalloidin (second row) or B2C that recognizes CT (third row). No model HBs were observed. Scale bar = 10 μm.

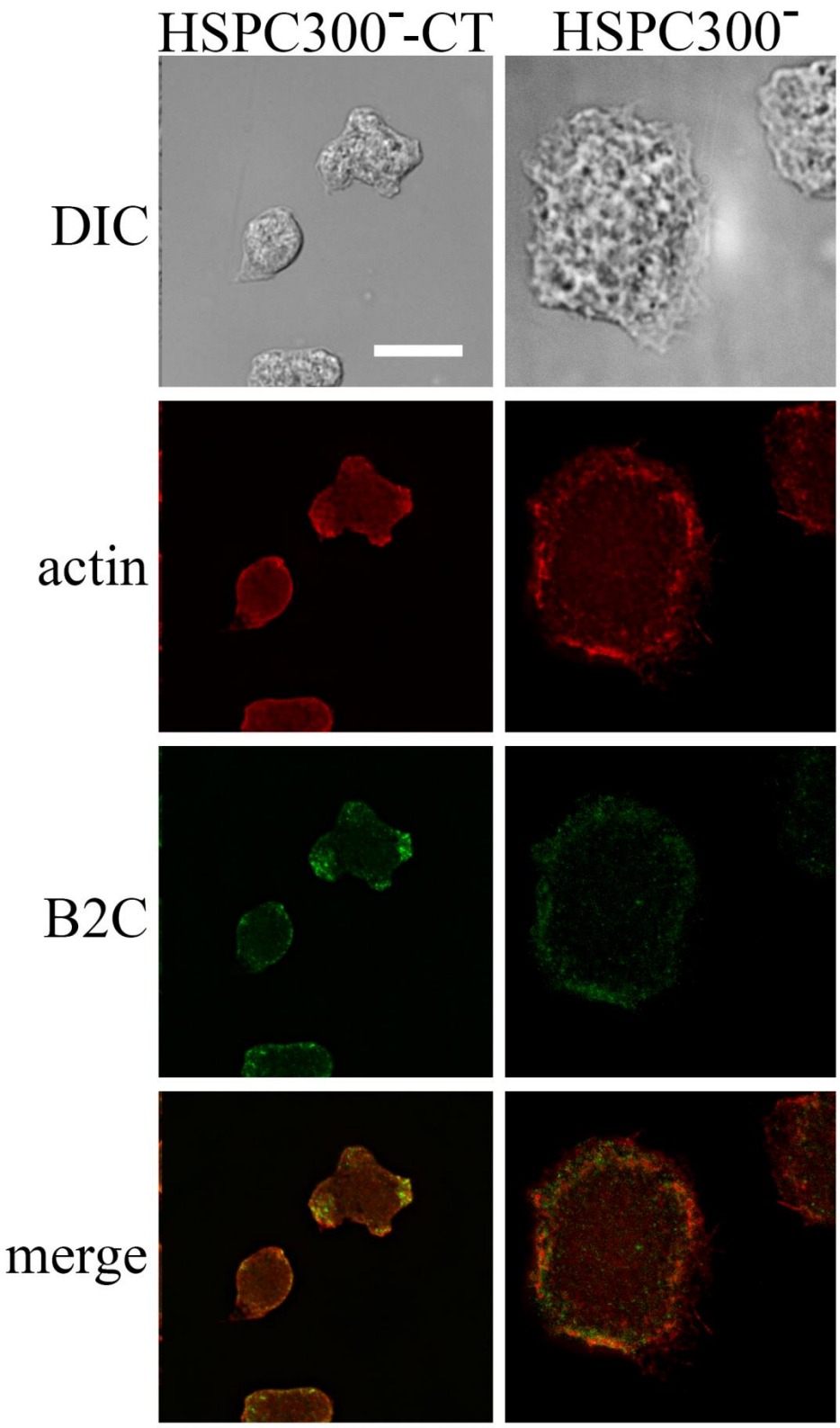
HSPC300⁻-CT
HSPC300⁻
DIC
actin
B2C
merge

Figure 2.11. Model HBs form in WshA$^-$-CT-myc. WshA$^-$ transformed with CT-myc (left panel), and untransformed WshA$^-$ (right panel), were examined by DIC microscopy (first row from the top), and by fluorescence microscopy using TRITC-phalloidin to stain F-actin (second row) or B2C that recognizes CT (third row). Model HBs enriched with CT were found in transformed cells. Scale bar = 10 μm.

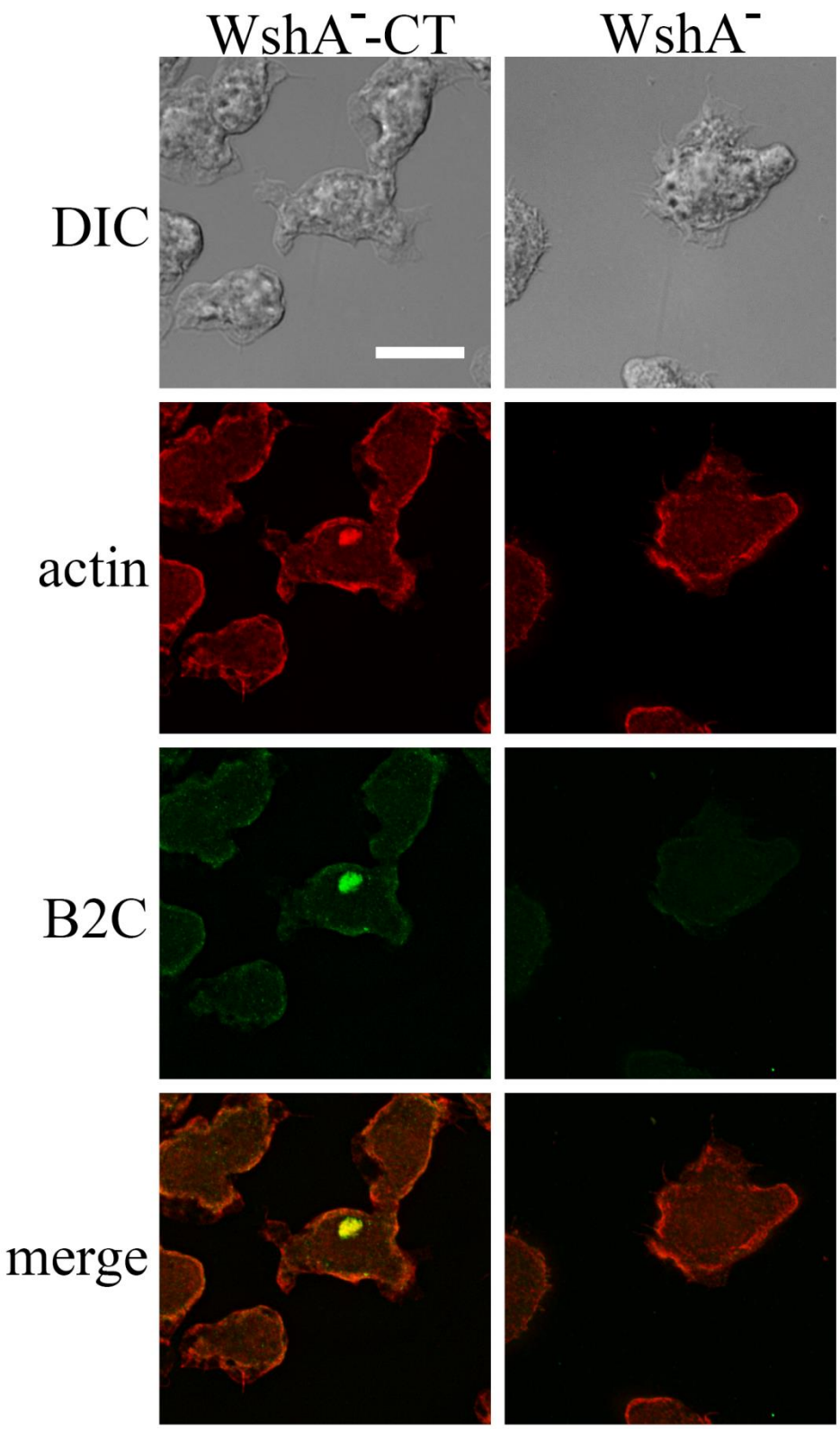
WshA⁻-CT
WshA⁻
DIC
actin
B2C
merge

Figure 2.12. Localization of Profilin I and F-actin in *Dictyostelium* cells generating model HBs. Cells expressing CT-myc were observed by DIC microscopy (A), and by fluorescence microscopy using either TRITC-phalloidin to stain F-actin (C) or antibody against profilin I followed by FITC-conjugated secondary antibody (D). Profilin I is enriched in model HBs (B, D). Scale bar = 10 μm.

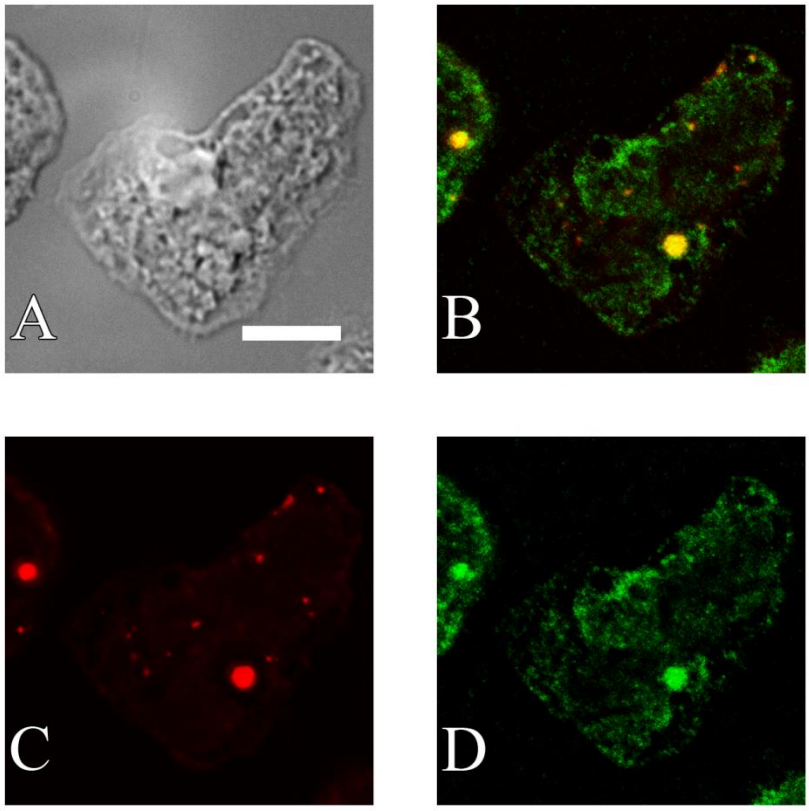
A
B
C
D

Figure 2.13. Model HBs form in profilin I knocked down cells. [AS]proA transformed with CT-myc were examined by DIC microscopy (A), and by fluorescence microscopy using TRITC-phalloidin to stain F-actin (C) or B2C that recognizes CT (D). Model HBs, which are actin aggregations enriched with CT, were found in transformed cells. Scale bar = 10 μm.

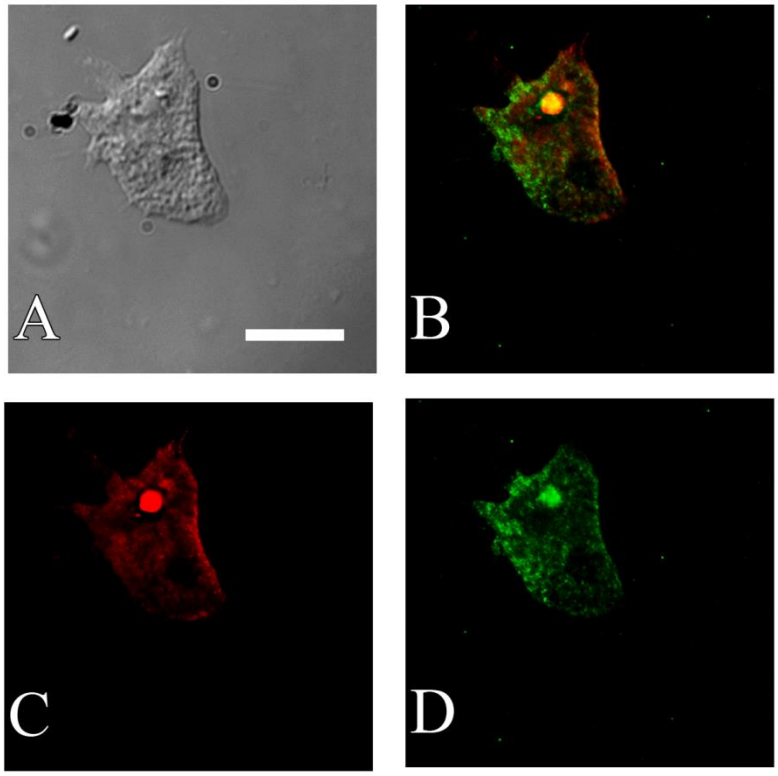
A
B
C
D

Figure. 2.14. Profilin I affects the size of model HBs. The size of model HBs were measured in [AS]proA-CT-myc and CT-myc cells in 3 independent experiments. A representative plot is shown. The size of model HBs significantly decreased when profilin I was knocked down ($p < 0.001$ for all 3 experiments).

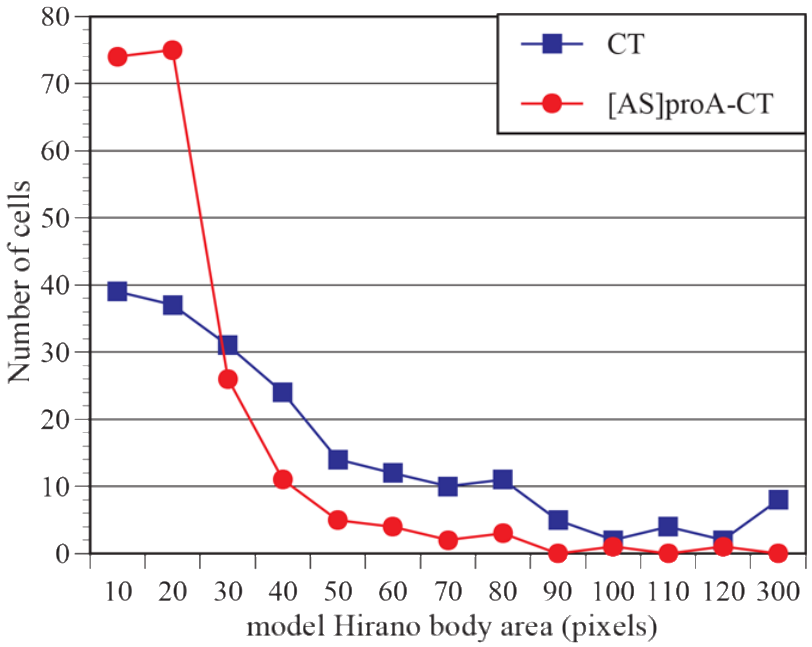
80
70
60
50
40
30
20
10
0
Number of cells
CT
[AS]proA-CT
10 20 30 40 50 60 70 80 90 100 110 120 300
model Hirano body area (pixels)

CHAPTER 3

CONCLUSION

In this study, I have investigated the roles of the proteins that regulate actin polymerization in model Hirano body formation. The candidates were selected based on the proteins identified by mass spectrometry on model Hirano bodies purified by density gradient [Shahid-Salles, Furukawa, Wells and Fechheimer, unpublished]. These candidates include subunits of the Arp2/3 complex Arp2 and Arp3, the activators of the Arp2/3 complex HSPC300 and WASH, and profilin. These proteins were shown to be colocalized with model HBs. Inhibition of the Arp2/3 complex activity led to a dramatic reduction of model HBs, and corresponding change in the distribution of model HB sizes. No model HBs were found when HSPC300 knockout was transformed with CT-myc, while some were found in transformed WASH knockout. CT-myc transformed into profilin knockdown cells generated model HBs, with a decreased size distribution. Considering the role of the Arp2/3 complex in actin nucleation and that of profilin in actin nucleotide exchange, these results suggest that de novo actin polymerization is crucial for Hirano body formation. However, discovery of this new aspect of Hirano body formation is not a final answer, but leads to more questions.

The Arp2/3 complex was investigated because of its presence in purified model HBs and also its role in actin nucleation [50, 52, 53]. The Arp2/3 complex enables the generation of daughter filament on side of a pre-existing mother filament with a 70 ° angle [52, 53], and thus the formation of an F-actin network [53]. HSPC300, as one subunit of the WAVE Regulatory Complex, functions in activation of the Arp2/3 complex [111]. Our results suggest that the

activation of the Arp2/3 complex by the WRC is necessary for model HB formation. However, this does not necessarily show that the WRC is an initiating factor in the process of generating model HBs. To address this question, the expression level of these proteins in model HB-producing cells should be tested. In addition, an investigation of model HB formation with gain of function forms or mutants which lead to differential functions of these proteins would be informative. If these proteins were shown upregulated in model HB producing-cells compared to the wild type, and larger model HBs were found with upregulating of these proteins, it would be more probable that Hirano body formation is initiated through this pathway.

Our results on the Arp2/3 complex and WRC also imply that their upstream regulators could as well play a role in Hirano body formation. The small GTPase Rac1 has been shown as one of the primary activators of WRC [61, 114] and is among the proteins identified with mass spectrometry on model HBs. Therefore, expression and/or activity of Rac1 should be tested when model HBs are induced, and observation of model HB formation when Rac1 activity is manipulated would be helpful in the characterization of the initiation of model HBs. However, WRC has been shown to be a scaffold, upon which multiple signals are integrated and coordinated [61, 122]. It is also likely that WRC's association with model HB formation merely represents this integration of complicated signals, and a global change on actin cytoskeleton. WAVE was found upregulated in plaque neurites of brain autopsy on AD patients [117], and in brains of 3xTg-AD mice with Aβ and tau pathology [116]. Moreover, Aβ was shown to stimulate actin polymerization in hippocampal neurons through Rac1 and Cdc42 [115]. Taken this together, it is possible that Aβ is among the signals that lead to Hirano body formation through WRC. To test this hypothesis, examination of size and frequency of the model HBs with Aβ or tau

stimulation is necessary. This is better carried out in mammalian cells, since the pathways that interact with Aβ are more likely to present in mammalian cell lines.

The role of profilin I was also investigated in this study. Our results suggest that profilin I enhances model HB formation, implying that profilin I might cooperate with the Arp2/3 complex in enhancing Hirano body formation. However, it has been shown that profilin indirectly inhibits the nucleation activity of the Arp2/3 complex by competing for G-actin with NPFs [67, 68]. Meanwhile, profilin directs G-actin to formins [67, 119, 120] or Ena/VASP [68]. In addition, targeting VASP to endosomes also induces the formation of giant F-actin aggregates, though the ultrastructure of these aggregates was shown to be disorganized [123]. Comparing these with our results, it implies that formins or Ena/VASP might also be critical in Hirano body formation, and that profilin ensures this coordination between the two systems. To verify this hypothesis, formins and VASP should be characterized in model HB generating cells. Knockout or overexpression cell lines of formins or VASP should be transformed with CT or E60K constructs, and if model HBs formed, their size and numbers should be quantified. This should test whether model HB formation in formin knockouts phenocopy that in profilin I knockdown cells. Colocalization of formins or VASP with model HBs should also be verified both in wild type cells and profilin I knock down cells to affirm that profilin I affects model HB formation through formins or VASP. Also, truncated forms of VASP that contain different functional domains could be expressed to examine how they affect HB formation.

In conclusion, this study reveals actin polymerization as a key aspect of Hirano body formation, in addition to the previously studied F-actin bundling and stabilization. This is also the first investigation of Hirano body formation studying the potential mechanisms of actin polymerization regulation. This suggests that Hirano body formation might be caused by a global

change in the actin cytoskeleton. Our data suggests that Hirano bodies may be a cellular response in the change of actin cytoskeleton induced by the pathogenesis of Alzheimer's disease.

REFERENCES

1. Glenner, G.G. and Wong, C.W., *Alzheimer's disease: initial report of the purification and characterization of a novel cerebrovascular amyloid protein.* Biochem. Biophys. Res. Commun., 1984. **120**: 885-90.
2. Kosik, K.S., Joachim, C.L., and Selkoe, D.J., *Microtubule-associated protein τ (tau) is a major antigenic component of paired helical filaments in Alzheimer's disease.* Proc. Natl. Acad. Sci. U. S. A., 1986. **83**: 4044-8.
3. Spillantini, M.G., Crowther, R.A., Jakes, R., Hasegawa, M., and Goedert, M., *α-synuclein in filamentous inclusions of Lewy bodies from Parkinson's disease and dementia with Lewy bodies.* Proc. Natl. Acad. Sci. U. S. A., 1998. **95**: 6469-73.
4. Neumann, M., Sampathu, D.M., Kwong, L.K., Truax, A.C., Micsenyi, M.C., Chou, T.T., Bruce, J., Schuck, T., Grossman, M., Clark, C.M., McCluskey, L.F., Miller, B.L., Masliah, E., Mackenzie, I.R., Feldman, H., Feiden, W., Kretzschmar, H.A., Trojanowski, J.Q., and Lee, V.M., *Ubiquitinated TDP-43 in frontotemporal lobar degeneration and amyotrophic lateral sclerosis.* Science, 2006. **314**: 130-3.
5. Guo, J.L. and Lee, V.M., *Cell-to-cell transmission of pathogenic proteins in neurodegenerative diseases.* Nat. Med., 2014. **20**: 130-8.
6. Guo, J.L. and Lee, V.M., *Seeding of normal Tau by pathological Tau conformers drives pathogenesis of Alzheimer-like tangles.* J. Biol. Chem., 2011. **286**: 15317-31.
7. Meyer-Luehmann, M., Coomaraswamy, J., Bolmont, T., Kaeser, S., Schaefer, C., Kilger, E., Neuenschwander, A., Abramowski, D., Frey, P., Jaton, A.L., Vigouret, J.M., Paganetti,

P., Walsh, D.M., Mathews, P.M., Ghiso, J., Staufenbiel, M., Walker, L.C., and Jucker, M., *Exogenous induction of cerebral β-amyloidogenesis is governed by agent and host.* Science, 2006. **313**: 1781-4.

8. Masuda-Suzukake, M., Nonaka, T., Hosokawa, M., Oikawa, T., Arai, T., Akiyama, H., Mann, D.M., and Hasegawa, M., *Prion-like spreading of pathological α-synuclein in brain.* Brain, 2013. **136**: 1128-38.
9. Hirano, A., Dembitzer, H.M., Kurland, L.T., and Zimmerman, H.M., *The fine structure of some intraganlionic alterations.* J. Neuropathol. Expt. Neurol., 1968. **27**: 167-82.
10. Gibson, P.H. and Tomlinson, B.E., *Numbers of Hirano bodies in the hippocampus of normal and demented people with Alzheimer's disease.* J. Neurol. Sci., 1977. **33**: 199-206.
11. Schmidt, M.L., Lee, V.M., and Trojanowski, J.Q., *Analysis of epitopes shared by Hirano bodies and neurofilament proteins in normal and Alzheimer's disease hippocampus.* Lab Invest, 1989. **60**: 513-22.
12. Schochet, S.S., Jr., Lampert, P.W., and Lindenberg, R., *Fine structure of the Pick and Hirano bodies in a case of Pick's disease.* Acta Neuropathol (Berl), 1968. **11**: 330-7.
13. Field, E.J. and Narang, H.K., *An electron-microscopic study of scrapie in the rat: further observations on "inclusion bodies" and virus-like particles.* J. Neurol. Sci., 1972. **17**: 347-64.
14. Tomonaga, M., *Hirano body in extraocular muscle.* Acta Neuropathol, 1983. **60**: 309-13.
15. Goldman, J.E., *The association of actin with Hirano bodies.* J Neuropathol Exp Neurol, 1983. **42**: 146-52.
16. Schochet, S.S., Jr. and McCormick, W.F., *Ultrastructure of Hirano bodies.* Acta Neuropathol, 1972. **21**: 50-60.

17. Griffin, P., Furukawa, R., Piggott, C., Maselli, A., and Fechheimer, M., *Requirements for Hirano Body formation.* Eukaryot. Cell, 2014. **13**: 625-34.

18. Bamburg, J.R. and Bloom, G.S., *Cytoskeletal pathologies of Alzheimer's disease.* Cell Motil. Cytoskeleton, 2009. **66**: 635-49.

19. McGough, A. and Chiu, W., *ADF/cofilin weakens lateral contacts in the actin filament.* J. Mol. Biol., 1999. **291**: 513-9.

20. Chan, C., Beltzner, C.C., and Pollard, T.D., *Cofilin dissociates Arp2/3 complex and branches from actin filaments.* Curr. Biol., 2009. **19**: 537-45.

21. Chen, H., Bernstein, B.W., Sneider, J.M., Boyle, J.A., Minamide, L.S., and Bamburg, J.R., *In vitro activity differences between proteins of the ADF/cofilin family define two distinct subgroups.* Biochemistry, 2004. **43**: 7127-42.

22. Andrianantoandro, E. and Pollard, T.D., *Mechanism of actin filament turnover by severing and nucleation at different concentrations of ADF/cofilin.* Mol. Cell, 2006. **24**: 13-23.

23. McGough, A., Pope, B., Chiu, W., and Weeds, A., *Cofilin changes the twist of F-actin: implications for actin filament dynamics and cellular function.* J. Cell Biol., 1997. **138**: 771-81.

24. Minamide, L.S., Striegl, A.M., Boyle, J.A., Meberg, P.J., and Bamburg, J.R., *Neurodegenerative stimuli induce persistent ADF/cofilin-actin rods that disrupt distal neurite function.* Nat. Cell Biol., 2000. **2**: 628-36.

25. Nishida, E., Iida, K., and Yonezawa, N., *Cofilin is a component of intranuclear and cytoplasmic actin rods induced in cultured cells.* Proc. Natl. Acad. Sci. U. S. A., 1987. **84**: 5262-6.

26. Maloney, M.T., Minamide, L.S., Kinley, A.W., Boyle, J.A., and Bamburg, J.R., *β-secretase-cleaved amyloid precursor protein accumulates at actin inclusions induced in neurons by stress or amyloid β: a feedforward mechanims for Alzheimer's disease.* J. Neurosci. Res., 2005. **25**: 11313-21.

27. Gessaga, E.C. and Anzil, A.P., *Rod-shaped filamentous inclusions and other ultrastructural features in a cerebellar astrocytoma.* Acta Neuropathol., 1975. **33**: 119-27.

28. Tomonaga, M., *Ultrastructure of Hirano bodies.* Acta Neuropathol, 1974. **28**: 365-6.

29. Maselli, A.G., Davis, R., Furukawa, R., and Fechheimer, M., *Formation of Hirano bodies in Dictyostelium and mammalian cells induced by expression of a modified form of an actin cross-linking protein.* J. Cell Sci., 2002. **115**: 1939-52.

30. Davis, R.C., Furukawa, R., and Fechheimer, M., *A cell culture model for investigation of Hirano bodies.* Acta Neuropathol., 2008. **115**: 205-17.

31. Ha, S., Furukawa, R., Stramiello, M., Wagner, J., and Fechheimer, M., *Transgenic mouse model for the formation of Hirano bodies.* BMC Neurosci., 2011. **12**: 97-112.

32. Furgerson, M., Clark, J.K., Crystal, J.D., Wagner, J., Fechheimer, M., and Furukawa, R., *Hirano body expression impairs spatial working memory in a novel mouse model.* Acta Neuropathol. Commun., 2014. **2**: 131-53.

33. Fechheimer, M. and Taylor, D.L., *Isolation and characterization of a 30,000-dalton calcium-sensitive actin cross-linking protein from Dictyostelium discoideum.* J. Biol. Chem., 1984. **259**: 4514-20.

34. Fechheimer, M., Murdock, D., Carney, M., and Glover, C.V.C., *Isolation and sequencing of cDNA clones encoding the Dictyostelium discoideum 30,000-dalton actin-bundling protein.* J. Biol. Chem., 1991. **266**: 2883-9.

35. Lim, R.W.L., Furukawa, R., Eagle, S., Cartwright, R.C., and Fechheimer, M., *Three distinct F-actin binding sites in the Dictyostelium discoideum 34,000 dalton actin bundling protein.* Biochemistry, 1999a. **38**: 800-12.

36. Lim, R.W.L., Furukawa, R., and Fechheimer, M., *Evidence of intramolecular regulation of the Dictyostelium discoideum 34,000 dalton F-actin bundling protein.* Biochemistry, 1999b. **38**: 16323-32.

37. Furukawa, R., Maselli, A.G., Thomson, S.A.M., Lim, R.W.-L., Stokes, J.V., and Fechheimer, M., *Calcium regulation of actin cross-linking is important for function of the actin cytoskeleton in Dictyostelium.* J. Cell Sci., 2003. **116**: 187-96.

38. Maselli, A.G., Furukawa, R., Thomson, S.A.M., Davis, R.C., and Fechheimer, M., *Formation of Hirano bodies induced by expression of an actin cross-linking protein with a gain of function mutation.* Eucaryot. Cell, 2003. **2**: 778-87.

39. Ha, S., Furukawa, R., and Fechheimer, M., *Association of AICD and Fe65 with Hirano bodies reduces transcriptional activation and initiation of apoptosis.* Neurobiol. Aging, 2011. **32**: 2287-98.

40. Kinoshita, A., Whelan, C.M., Berezovska, O., and Hyman, B.T., *The gamma secretase-generated carboxyl-terminal domain of the amyloid precursor protein induces apoptosis via Tip60 in H4 cells.* J. Biol. Chem., 2002. **277**: 28530-6.

41. Kinoshita, A., Whelan, C.M., Smith, C.J., Berezovska, O., and Hyman, B.T., *Direct visualization of the gamma secretase-generated carboxyl-terminal domain of the amyloid precursor protein: association with Fe65 and translocation to the nucleus.* J. Neurochem., 2002. **82**: 839-47.

42. Lu, D.C., Soriano, S., Bredesen, D.E., and Koo, E.H., *Caspase cleavage of the amyloid precursor protein modulates amyloid beta-protein toxicity.* J. Neurochem., 2003. **87**: 733-41.

43. Furgerson, M., Fechheimer, M., and Furukawa, R., *Model Hirano bodies protect against tau-independent and tau-dependent cell death initiated by the amyloid precursor protein intracellular domain.* PLoS One, 2012. **7**: e44996.

44. Spears, W., Furgerson, M., Sweetnam, J.M., Evans, P., Gearing, M., Fechheimer, M., and Furukawa, R., *Hirano bodies differentially modulate cell death induced by tau and the amyloid precursor protein intracellular domain.* BMC Neurosci., 2014. **15**: 74.

45. Kim, D.H., Davis, R.C., Furukawa, R., and Fechheimer, M., *Autophagy contributes to degradation of Hirano bodies.* Autophagy, 2009. **5**: 44-51.

46. Gomez, T.M. and Letourneau, P.C., *Actin dynamics in growth cone motility and navigation.* J. Neurochem., 2014. **129**: 221-34.

47. Insall, R.H. and Machesky, M., *Actin dynamics at the leading edge: from simple machinery to complex networks.* Dev. Cell, 2009. **17**: 310-22.

48. Moore, P.B., Huxley, H.E., and DeRosier, D.J., *Three-dimensional reconstruction of F-actin, thin filaments and decorated thin filaments.* J. Mol. Biol., 1970. **50**: 279-95.

49. Pollard, T.D., *Rate constants for the reactions of ATP- and ADP-actin with the ends of actin filaments.* J. Cell Biol., 1986. **103**: 2747-54.

50. Firat-Karalar, E.N. and Welch, M., *New mechanisms and functions of actin nucleation.* Curr. Opin. Cell Biol., 2011. **23**: 4-13.

51. Machesky, L.M. and Gould, K.L., *The Arp2/3 complex: a multifunctional actin organizer.* Curr. Opin. Cell Biol., 1999. **11**: 117-21.

52. Rouiller, I., Xu, X., Amann, K.J., Egile, C., Nickell, S., Nicastro, D., Li, R., Pollard, T.D., Volkmann, N., and Hanein, D., *The structural basis of actin filament branching by the Arp2/3 complex.* J. Cell Biol., 2008. **180**: 887-95.

53. Mullins, R.D., Heuser, J.A., and Pollard, T.D., *The interaction of Arp2/3 complex with actin: nucleation, high affinity pointed end capping, and formation of branching networks of filaments.* Proc. Natl. Acad. Sci. U. S. A., 1998. **95**: 6181-6.

54. Boczkowsa, M., Rebowski, G., Petoukhov, M.V., Hayes, D.B., Svergun, D.I., and Dominguez, R., *X-ray scattering study of activated Arp2/3 complex with bound actin-WCA.* Structure, 2008. **16**: 695-704.

55. Goley, E.D. and Welch, M.D., *The ARP2/3 complex: an actin nucleator comes of age.* Nat. Rev. Mol. Cell Biol., 2006. **7**: 713-26.

56. Le Clainche, C. and Carlier, M.F., *Regulation of actin assembly associated with protrusion and adhesion in cell migration.* Physiol. Rev., 2008. **88**: 489-513.

57. Goley, E.D., Rodenbusch, S.E., Martin, A.C., and Welch, M.D., *Critical conformational changes in the Arp2/3 complex are induced by nucleotide and nucleation promoting factor.* Mol. Cell, 2004. **16**: 269-79.

58. Zalevsky, J., Lempert, L., Kranitz, H., and Mullins, R.D., *Different WASP family proteins stimulate different Arp2/3 complex-dependent actin-nucleating activities.* Curr. Biol., 2001. **11**: 1903-13.

59. Tomasevic, N., Jia, Z., Russell, A., Fujii, T., Hartman, J.J., Clancy, S., Wang, M., Beraud, C., Wood, K.W., and Sakowicz, R., *Differential regulation of WASP and N-WASP by Cdc42, Rac1, Nck, and PI(4,5)P_2.* Biochemistry, 2007. **46**: 3494-502.

60. Chen, Z., Borek, D., Padrick, S.B., Gomez, T.S., Metlagel, Z., Ismail, A.M., Umetani, J., Billadeau, D.D., Otwinowski, Z., and Rosen, M.K., *Structure and control of the actin regulatory WAVE complex.* Nature, 2010. **468**: 533-8.

61. Chen, B., Brinkmann, K., Chen, Z., Pak, C., Liao, Y., Shi, S., Henry, L., Grishin, N., Bogdan, S., and Rosen, M., *The WAVE regulatory complex links diverse receptors to the actin cytoskeleton.* Cell, 2014. **156**: 195-207.

62. Yarar, D., D'Alessio, J., Jeng, R., and Welch, M., *Motility determinants in WASP family proteins.* Mol. Biol. Cell, 2002. **13**: 4045.

63. Tilney, L.G., *The polymerization of actin. V. A new organelle, the actomere, that initiates the assembly of actin filaments in Thyone sperm.* J. Cell Biol., 1978. **77**: 551-64.

64. Perelroizen, I., Carlier, M.F., and Pantaloni, D., *Binding of divalent cation and nucleotide to G-actin in the presence of profilin.* . J. Biol. Chem., 1995. **270**: 1501-8.

65. Selden, L.A., Kinosian, H.J., Estes, J.E., and Gershman, L.C., *Impact of profilin on actin-bound nucleotide exchange and actin polymerization dynamics.* Biochemistry, 1999. **38**: 2769-78.

66. Minehardt, T.J., Kollman, P.A., Cooke, R., and Pate, E., *The open nucleotide pocket of the profilin/actin X-ray structure is unstable and closes in the absence of profilin.* Biophys. J., 2006. **90**: 2445-9.

67. Suarez, C., Carroll, R., Burke, T., Christensen, J., Bestul, A., Sees, J., James, M., Sirotkin, V., and Kovar, D., *Profilin regulates F-Actin network homeostasis by favoring formin over Arp2/3 complex.* Dev. Cell, 2015. **32**: 43-53.

68. Rotty, J., Wu, C., Haynes, E., Suarez, C., Winkelman, J., Johnson, H., Haugh, J., Kovar, D., and Bear, J., *Profilin-1 serves as a gatekeeper for actin assembly by Arp2/3-dependent and -independent pathways.* Dev. Cell, 2015. **32**: 54-67.

69. Jockusch, B.M., Murk, K., and Rothkegel, M., *The profile of profilins.* Rev. Physiol. Biochem. Pharmacol., 2007. **159**: 131-49.

70. Pollard, T.D. and Cooper, J.A., *Quantitative analysis of the effect of Acanthamoeba profilin on actin filament nucleation and elongation.* Biochemistry, 1984. **23**: 6631-41.

71. Galloway, P.G., Perry, G., and Gambetti, P., *Hirano body filaments contain actin and actin-associated proteins.* J. Neuropathol. Exp. Neurol., 1987. **46**: 185-99.

72. Peress, N.S. and Perillo, E., *Differential expression of TFG Beta 1, 2, and 3 isotypes in Alzheimer's disease: a comparative immunohistochemical study with cerebral infarction, aged human and mouse control brainsq.* J. Neuropathol. Exp. Neurol., 1995. **54**: 802-11.

73. Singhrao, S.K., *C1q, the classical complement pathway protein binds Hirano bodies in Pick's disease.* Microsc. Res. Tech., 2013. **76**: 606-11.

74. Satoh, J., Tabunoki, H., Ishida, T., Saito, Y., and Arima, K., *Ubiquilin-1 immunoreactivity is concentrated on Hirano bodies and dystrophic neurites in Alzheimer's disease brains.* Neuropathol. Appl. Neurobiol., 2013. **39**: 817-30.

75. Rossiter, J.P., Anderson, L.L., Yang, F., and Cole, G.M., *Caspase-cleaved actin (fractin) immunolabelling of Hirano bodies.* Neuropathol. Appl. Neurobiol., 2000. **26**: 342-6.

76. Kokoulina, P. and Rohn, T.T., *Caspase-cleaved transactivation response DNA-binding protein 43 in Parkinson's disease and dementia with Lewy bodies.* Neurodegener. Dis., 2010. **7**: 243-50.

77. Zhu, X., Raina, A.K., Rottkamp, C.A., Aliev, G., Perry, G., Boux, H., and Smith, M.A., *Activation and redistribution of c-jun N-terminal kinase/stress activated protein kinase in degenerating neurons in Alzheimer's disease.* J. Neurochem., 2001. **76**: 435-41.

78. Santa-Maria, I., Santpere, G., MacDonald, M.J., de Barreda, E.G., Hernandez, F., Moreno, F.J., Ferrer, I., and Avila, J., *Coenzyme Q induces tau aggregation, tau filaments, and Hirano bodies.* J. Neuropathol. Exp. Neurol., 2008. **67**: 428-34.

79. Maciver, S.K. and Harrington, C.R., *Two actin binding proteins, actin depolymerizing factor and cofilin, are associated with Hirano bodies.* Neuroreport, 1995. **6**: 1985-8.

80. Munoz, D.G., Wang, D., and Greenberg, B.D., *Hirano bodies accumulate C-terminal sequences of β-amyloid precursor protein (β-APP) epitopes.* J. Neuropathol. Exp. Neurol., 1993. **52**: 14-21.

81. Cao, X. and Südhof, T.C., *A transcriptionally active complex of APP with Fe65 and histone acetyltransferase Tip60.* Science, 2001. **293**: 115-20.

82. Jordan-Sciutto, K., Dragich, J., Walcott, D., and Bowser, R., *The presence of FAC1 protein in Hirano bodies.* Neuropathol. Appl. Neurobiol., 1998. **24**: 359-66.

83. Kon, T., Mori, F., Tanji, K., Miki, Y., Toyoshima, Y., Yoshida, M., Sasaki, H., Kakita, A., Takahashi, H., and Wakabayashi, K., *ALS-associated protein FIG4 is localized in Pick and Lewy bodies, and also neuronal nuclear inclusions, in polyglutamine and intranuclear inclusion body diseases.* Neuropathology, 2014. **34**: 19-26.

84. Lee, H.G., Ueda, M., Miyamoto, Y., Yoneda, Y., Perry, G., Smith, M.A., and Zhu, X., *Aberrant localization of importin a1 in hippocampal neurons in Alzheimer disease.* Brain Res., 2006. **1124**: 1-4.

85. Lee, S.C., Zhao, M.L., Hirano, A., and Dickson, D.W., *Inducible nitric oxide synthase immunoreactivity in the Alzheimer disease hippocampus: association with Hirano bodies, neurofibrillary tangles, and senile plaques.* J. Neuropathol. Exp. Neurol., 1999. **58**: 1163-9.

86. Perry, G., Zhu, X., Babar, A.K., Siedlak, S.L., Yang, Q., Ito, G., Iwatsubo, T., Smith, M.A., and Chen, S.G., *Leucine-rich repeat kinase 2 colocalizes with alpha-synuclein in Parkinson's disease, but not tau-containing deposits in tauopathies.* Neurodegener. Dis., 2008. **5**: 222-4.

87. Gong, H., Dong, W., Rostad, S.W., Marcovina, S.M., Albers, J.J., Brunzell, J.D., and Vuletic, S., *Lipoprotein lipase (LPL) is associated with neurite pathology and its levels are markedly reduced in the dentate gyrus of Alzheimer's disease brains.* J. Histochem. Cytochem, 2013. **61**: 857-68.

88. Peterson, C., Kress, Y., Vallee, R., and Goldman, J.E., *High molecular weight microtubule-associated proteins bind to actin lattices (Hirano bodies).* Acta Neuropathol., 1988. **77**: 168-74.

89. Previll, L.A., Crosby, M.E., Castellani, R.J., Bowser, R., Perry, G., Smith, M.A., and Zhu, X., *Increased expression of p130 in Alzheimer's disease.* Neurochem. Res., 2007. **32**: 639-44.

90. Shao, C.Y., Mirra, S.S., Sait, H.B., Sacktor, T.C., and Sigurdsson, E.M., *Postsynaptic degeneration as revealed by PSD-95 reduction occurs after advanced Aβ and tau pathology in transgenic mouse models of Alzheimer's disease.* Acta Neuropathol., 2011. **122**: 285-92.

91. Makioka, K., Yamazaki, T., Takatama, M., Ikeda, M., and Okamoto, K., *Immunolocalization of Smurf1 in Hirano bodies.* J. Neurol. Sci., 2014. **336**: 24-8.

92. Renkawek, K., Bosman, G.J., and de Jong, W.W., *Expression of small heat-shock protein hsp 27 in reactive gliosis in Alzheimer disease and other types of dementia.* Acta Neuropathol., 1994. **87**: 511-9.

93. Hong, Y., Chan, C.B., Kwon, I.S., Li, X., Song, M., Lee, H.P., Liu, X., Sompol, P., Jin, P., Lee, H.G., Yu, S.P., and Ye, K., *SRPK2 phosphorylates tau and mediates the cognitive defects in Alzheimer's disease.* J. Neurosci., 2012. **32**: 17262-72.

94. Galloway, P.G., Perry, G., Kosik, K.S., and Gambetti, P., *Hirano bodies contain tau protein.* Brain Res., 1987. **403**: 337-40.

95. Rohn, T.T., *Caspase-cleaved TAR DNA-binding protein-43 is a major pathological finding in Alzheimer's disease.* Brain Res., 2008. **1228**: 189.

96. Rohn, T.T. and Kokoulina, P., *Caspase-cleaved TAR DNA-binding protein-43 in Pick's disease.* Int. J. Physiol. Pathophysiol. Pharmacol., 2009. **1**: 25-32.

97. Davis, R.C., Maloney, M.T., Minamide, L.S., Flynn, K.C., Stonebraker, M.A., and Bamburg, J.R., *Mapping cofilin-actin rods in stressed hippocampal slices and the role of cdc42 in amyloid-β-induced rods.* J. Alzheimers Dis., 2009. **18**: 35-50.

98. Watts, D.J. and Ashworth, J.M., *Growth of myxamoebae of the cellular slime mould Dictyostelium discoideum in axenic culture.* Biochem. J., 1970. **119**: 171-4.

99. Blusch, J., Morandini, P., and Nellen, W., *Transcriptional regulation by folate: inducible gene expression in Dictyostelium transformants during growth and early development.* Nucl. Acids Res., 1992. **20**: 6235-8.

100. Loomis, W.F., *Sensitivity of Dictyostelium discoideum to nucleic acid analogues.* Exp. Cell Res., 1971. **64**: 484-6.

101. Witke, W., Nellen, W., and Noegel, A.A., *Homologous recombination in the Dictyostelium alpha-actinin gene leads to an altered mRNA and lack of protein.* EMBO J., 1987. **6**: 4143-8.

102. Rivero, F., Furukawa, R., Noegel, A.A., and Fechheimer, M., *Dictyostelium discoideum cells lacking the 34,000 dalton actin binding protein can grow, locomote, and develop, but exhibit defects in regulation of cell structure and movement: a case of partial redundancy.* J. Cell Biol., 1996. **135**: 965-80.

103. Fey, P., Dodson, R.J., Basu, S., and Chisholm, R.L., *One stop shop for everything Dictyostelium: dictyBase and the Dicty Stock Center in 2012.* Methods Mol. Biol., 2013. **983**: 59-92.

104. Fechheimer, M., *The Dictyostelium discoideum 30,000-dalton protein is an actin filament-bundling protein that is selectively present in filopodia.* J. Cell Biol., 1987. **104**: 1539-51.

105. Haugwitz, M., Noegel, A.A., Karakesisoglou, J., and Schleicher, M., *Dictyostelium amoebae that lack G-actin sequestering profilins show defects in F-actin content, cytokinesis, and development.* Cell, 1994. **79**: 303-14.

106. Schneider, C.A., Rasband, W.S., and Eliceiri, K.W., *NIH Image to ImageJ: 25 years of image analysis.* Nat. Methods, 2012. **9**: 671-5.

107. Insall, R.H., Müller-Taubenberger, A., Machesky, L., Köhler, J., Simmeth, E., Atkinson, S.J., Weber, I., and Geresch, G., *Dynamics of the Dictyostelium Arp2/3 complex in endocytosis, cytokinesis, and chemotaxis.* Cell Motil. Cytoskeleton, 2001. **50**: 115-28.

108. Nolen, B.J., Tomasevic, N., Russell, A., Pierce, D.W., Jia, Z., McCormick, C.D., Hartman, J., Sakowicz, R., and Pollard, T.D., *Characterization of two classes of small molecule inhibitors of Arp2/3 complex.* Nature, 2009. **460**: 1031-4.

109. Yang, Q., Zhang, X., Pollard, T.D., and Forscher, P., *Arp2/3 complex–dependent actin networks constrain myosin II function in driving retrograde actin flow.* J. Cell Biol., 2012. **197**: 939-56.

110. Reyes, J.F., Stone, K., Ramos, J., and Maselli, A., *Formation of Hirano bodies after inducible expression of a modified form of an actin-cross-linking protein.* Eukaryot. Cell, 2009. **8**: 6.

111. Pollitt, A.Y. and Insall, R.H., *Loss of Dictyostelium HSPC300 causes a scar-like phenotype and loss of SCAR protein.* BMC Cell Biol., 2009. **10**: 13.

112. Carnell, M., Zech, T., Calaminus, S.D., Ura, S., Hagedorn, M., Johnston, S.A., May, R.C., Soldati, T., Machesky, L., and Insall, R.H., *Actin polymerization driven by WASH causes V-ATPase retrieval and vesicle neutralization before exocytosis.* J. Cell Biol., 2011. **193**: 831-9.

113. Carasino, D., Jones, C., Compton, M., and Saxe, C.L.I., *The N-terminus of Dictyostelium Scar interacts with Abi and HSPC300 and is essential for proper regulation and function.* Mol. Biol. Cell, 2007. **18**: 1609-20.

114. Eden, S., Rohatgi, R., Podtelejnikov, A.V., Mann, M., and Kirschner, M.W., *Mechanism of regulation of WAVE1-induced actin nucleation by Rac1 and Nck.* Nature, 2002. **418**: 790-3.

115. Mendoza-Naranjo, A., Gonzalez-Billault, C., and Maccioni, R.B., *$A\beta_{1-42}$ stimulates actin polymerization in hippocampal neurons through Rac1 and Cdc42 Rho GTPases.* J. Cell Sci., 2007. **120**: 279-88.

116. Takata, K., Kitamura, Y., Nakata, Y., Matsuoka, Y., Tomimoto, H., Taniguchi, T., and Shimohama, S., *Involvement of WAVE accumulation in Aβ/APP pathology-dependent tangle modification in Alzheimer's disease.* Am. J. Pathol., 2009. **175**: 17-24.

117. Kitamura, Y., Tsuchiya, D., Takata, K., Shibagaki, K., Taniguchi, T., Smith, M.A., Perry, G., Miki, H., Takenawa, T., and Shimohama, S., *Possible involvement of Wiskott-Aldrich syndrome protein family in aberrant neuronal sprouting in Alzheimer's disease.* Neurosci. Lett., 2003. **346**: 149-52.

118. Perelroizen, I., Didry, D., Christensen, H., Chua, N., and Carlier, M., *Role of nucleotide exchange and hydrolysis in the function of profilin in actin assembly.* J. Biol. Chem., 1996. **271**: 12302-9.

119. Kovar, D.R., Kuhn, J.R., Tichy, A.L., and Pollard, T.D., *The fission yeast cytokinesis formin Cdc12p is a barbed end actin filament capping protein gated by profilin.* J. Cell Biol., 2003. **161**: 875-87.

120. Romero, S., Le Clainche, C., Didry, D., Egile, C., Pantaloni, D., and Carlier, M.F., *Formin is a processive motor that requires profilin to accelerate actin assembly and associated ATP hydrolysis.* Cell, 2004. **119**: 419-29.

121. Lázaro-Diéguez, F., Aguado, C., Mato, E., Sánchez-Ruiz, Y., Esteban, I., Alberch, J., Knecht, E., and Egea, G., *Dynamics of an F-actin aggresome generated by the actin-stabilizing toxin jasplakinolide.* J. Cell Sci., 2008. **121**: 1415-25.

122. Westphal, R.S., Soderling, S.H., Alto, N.M., Langeberg, L.K., and Scott, J.D., *Scar/WAVE-1, a Wiskott-Aldrich syndrome protein, assembles an actin-associated multi-kinase scaffold.* EMBO J., 2000. **19**: 4589-600.

123. Schmauch, C., Claussner, S., Zöltzer, H., and Maniak, M., *Targeting the actin-binding protein VASP to late endosomes induces the formation of giant actin aggregates.* Eur. J. Cell Biol., 2009. **88**: 385-96.